

上卷 卷之二
卷之二

卷之二 卷之二 卷之二 卷之二 卷之二 卷之二 卷之二 卷之二 卷之二 卷之二

卷之二

卷之二 卷之二 卷之二 卷之二 卷之二 卷之二 卷之二 卷之二 卷之二 卷之二

卷之二 卷之二 卷之二 卷之二 卷之二 卷之二 卷之二 卷之二 卷之二 卷之二

卷之二

卷之二

卷之二 卷之二 卷之二 卷之二 卷之二 卷之二 卷之二 卷之二 卷之二 卷之二

卷之二 卷之二 卷之二 卷之二 卷之二 卷之二 卷之二 卷之二 卷之二 卷之二

CR 4

REPORT
ON
THE MINERAL EXPLORATION
IN
THE PACHAPIRIANA AREA
REPUBLIC OF PERU

(PHASE III)

JICA LIBRARY

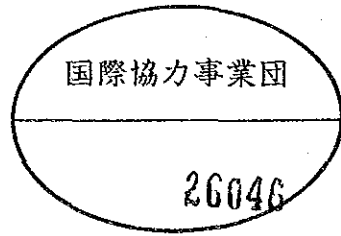


1111464121

26096

MARCH 1991

JAPAN INTERNATIONAL COOPERATION AGENCY
METAL MINING AGENCY OF JAPAN



Preface

In response to the request of the Government of the Republic of Peru, the Japanese Government decided to conduct a Mineral Exploration in the Pachapiriana Area Project and entrusted the survey to the Japan International Cooperation Agency(JICA) and the Metal Mining Agency of Japan(MMAJ).

The JICA and MMAJ sent to the Republic of Peru a survey team headed by Mr. Hiroshi Hama from July 7 to December 7, 1990. The team exchanged views with the officials concerned of the Government of the Republic of Peru and conducted a field survey in the Pachapiriana area. After the team returned to Japan, further studies were made and the present report has been prepared.

We hope that this report will serve for the development of the Project and contribute to the promotion of friendly relations between our two countries.

We wish to express our deep appreciation to the officials concerned of the Government of the Republic of Peru for their close cooperation extended to the team.

February, 1991



Kensuke YANAGIYA
President
Japan International Cooperation Agency



Gen-ichi Fukuhara
President
Metal Mining Agency of Japan

CONTENTS

Preface

Location Map of the Survey Area

Summary

PART I GENERAL REMARKS

CHAPTER 1 INTRODUCTION

- 1-1 Antecedents of the Survey
- 1-2 Conclusion and Recommendation of the Second Year Survey
- 1-3 Outline of the Third Year Survey

CHAPTER 2 GEOGRAPHY OF THE SURVEY AREA

- 2-1 Topography and Drainage System
- 2-2 Climate and Vegetation

CHAPTER 3 GENERAL GEOLOGY

CHAPTER 4 SURVEY RESULTS, COMPREHENSIVE ANALYSIS

- 4-1 Geological Structure, and Characteristics and Controlling Factors of the Mineralization
- 4-2 Potentiality of an Existence of Ore Deposits
- 4-3 Relation between Geochemical Anomaly and Mineralization

CHAPTER 5 CONCLUSION AND RECOMMENDATION

- 5-1 Conclusion
- 5-2 Recommendation for the Fourth Year Survey

PART II PARTICULARS

CHAPTER 1 CHONTALI AREA

- 1-1 Geophysical Survey
- 1-2 Drilling Survey
- 1-3 Consideration

CHAPTER 2 JEHUAMARCA AREA

- 2-1 Geological Survey and Geochemical Survey
- 2-2 Drilling Survey
- 2-3 Consideration

PART III CONCLUSION AND RECOMMENDATION

CHAPTER 1 CONCLUSION

CHAPTER 2 RECOMMENDATION FOR THE FOURTH YEAR SURVEY

REFERENCES

LIST OF FIGUERS

- Fig I-1 (1) Location and Accessibility of the Survey Area
Fig I-1 (2) Location of the Survey Area
Fig I-2 Summarized Accessibility of the Survey Area
Fig I-3 Generalized Geological Map of the Survey Area
Fig I-4 Generalized Stratigraphic Column of the Survey Area
Fig I-5 Distribution of Mineralization in the Survey Area
Fig II-1 Gravity Survey Area
Fig II-2 Location of Gravity Stations
Fig II-3 Annular Segment for Terrain Correction
Fig II-4 Division of Terrain Correction Area
Fig II-5 Gravity versus Height Relation
Fig II-6 Energy Spectrum
Fig II-7 Bouguer Anomaly Map ($\rho=2.67\text{g/cm}^3$)
Fig II-8 First-order Residual Gravity Map
Fig II-9 (1) Long-wave Gravity Map
Fig II-9 (2) Short-wave Gravity Map
Fig II-10 (1) Cross Section of A-A'
Fig II-10 (2) Cross Section of B-B'
Fig II-10 (3) Cross Section of C-C'
Fig II-10 (4) Cross Section of D-D'
Fig II-11 Geophysical Interpretation Map
Fig II-12 Location of the Drillings with showing Geophysical
Survy Results in the Chontali Area
Fig II-13 Interpretative Profiles of the Drilings
in the Chontali Area
Fig II-14 Assay Results on the Profiles of the Drillings
in the Chontali Area
Fig II-15 Distribution of Fluid Inclusion Homogenization
Temperaure in the Chontali Area
Fig II-16 Histogram and Cumulative Frequency Diagram of
Geochemical Data in the Jehuamarca Area
Fig II-17 Geological Map of the Jehuamarca Area
Fig II-18 Geological Profiles of the Jehuamarca Area
Fig II-19 (1) Distribution of Geochemical Anomaly
in the Jehuamarca Area (Au,Ag)

- Fig. II-19 (2) Distribution of Geochemical Anomaly
in the Jehuamarca Area (Cu, Pb and Zn)
- Fig. II-20 Location of the Drilling and Trenching Sites
in the Jehuamarca Area
- Fig. II-21 Assay Results on the Profiles of the Drillings
in the Jehuamarca Area
- Fig. III-1 Location of the Recommended Drilling Sites
in the Chontali Area

LIST OF TABLES

- Table II-1 Calculations of Gravity Standard Value
- Table II-2 Rock Properties
- Table II-3 List of Gravity Data
- Table II-4 Geochemical Threshold of the Jehuamarca Area
- Table III-1 Recommended Drilling Sites in the Chontali Area

LIST OF PLATES

PL -1	Location of Gravity Stations	scale 1/10,000
PL -2	Bouguer Anomaly Map ($\rho=2.67\text{g/cm}^3$)	scale 1/10,000
PL -3	First-order Residual Gravity Map	scale 1/10,000
PL -4 (1)	Long-wave Gravity Map	scale 1/10,000
PL -4 (2)	Short-wave Gravity Map	scale 1/10,000
PL -5 (1)	Cross Section of A-A'	scale 1/10,000
PL -5 (2)	Cross Section of B-B'	scale 1/10,000
PL -5 (3)	Cross Section of C-C'	scale 1/10,000
PL -5 (4)	Cross Section of D-D'	scale 1/10,000
PL -6	Geophysical Interpretation Map	scale 1/10,000
PL -7 (1)	Core Log (MJPC-1) Chontali Area	scale 1/200
PL -7 (2)	Core Log (MJPC-2) Chontali Area	scale 1/200
PL -7 (3)	Core Log (MJPC-3) Chontali Area	scale 1/200
PL -7 (4)	Core Log (MJPC-4) Chontali Area	scale 1/200
PL -7 (5)	Core Log (MJPC-5) Chontali Area	scale 1/200
PL -7 (6)	Core Log (MJPC-6) Chontali Area	scale 1/200
PL -8	Geological Map of the Jehuamarca Area	scale 1/2,500
PL -9	Geological Profiles of the Jehuamarca Area	scale 1/2,500
PL -10	Location Map of Samples in the Jehuamarca Area	scale 1/2,500
PL -11 (1)	Distribution of Geochemical Anomaly in the Jehuamarca Area (Au,Ag)	scale 1/2,500
PL -11 (2)	Distribution of Geochemical Anomaly in the Jehuamarca Area (Cu,Pb and Zn)	scale 1/2,500
PL -12 (1)	Core Log (MJPJ-4,5) Jehuamarca Area	scale 1/200
PL -12 (2)	Core Log (MJPJ-6,7) Jehuamarca Area	scale 1/200
PL -12 (3)	Core Log (MJPJ-8,9) Jehuamarca Area	scale 1/200
PL -12 (4)	Core Log (MJPJ-10,11) Jehuamarca Area	scale 1/200
PL -12 (5)	Core Log (MJPJ-12,13) Jehuamarca Area	scale 1/200

LIST OF APPENDIXES

- ApX. 1 Microscopic Observations of Thin Sections
- ApX. 2 Microscopic Photographs of Thin Sections
- ApX. 3 Results of Fluid Inclusion Homogenization Temperature Analysis
- ApX. 4 Results of X-ray diffractive Analysis
- ApX. 5 X-ray Diffraction Chart
- ApX. 6 Microscopic Observations of Polished Sections
- ApX. 7 Microscopic Photographs of Polished Sections
- ApX. 8 Assay Results of Drilling Core in the Chontali Area
- ApX. 9 Assay Results of Drilling Core in the Jehuamaca Area
- ApX. 10 Assay Results of Ore at Trench-1 in the Jehuamaca Area
- ApX. 11 Assay Results of Geochemical Samples
in the Jehuamaca Area
- ApX. 12 Geological Drilling Log in the Chontali Area
- ApX. 13 Geological Drilling Log in the Jehuamaca Area
- ApX. 14 Geological Sketches of Trenches in the Jehuamaca Area
- ApX. 15 Miscellaneous Data for the Drilling Survey

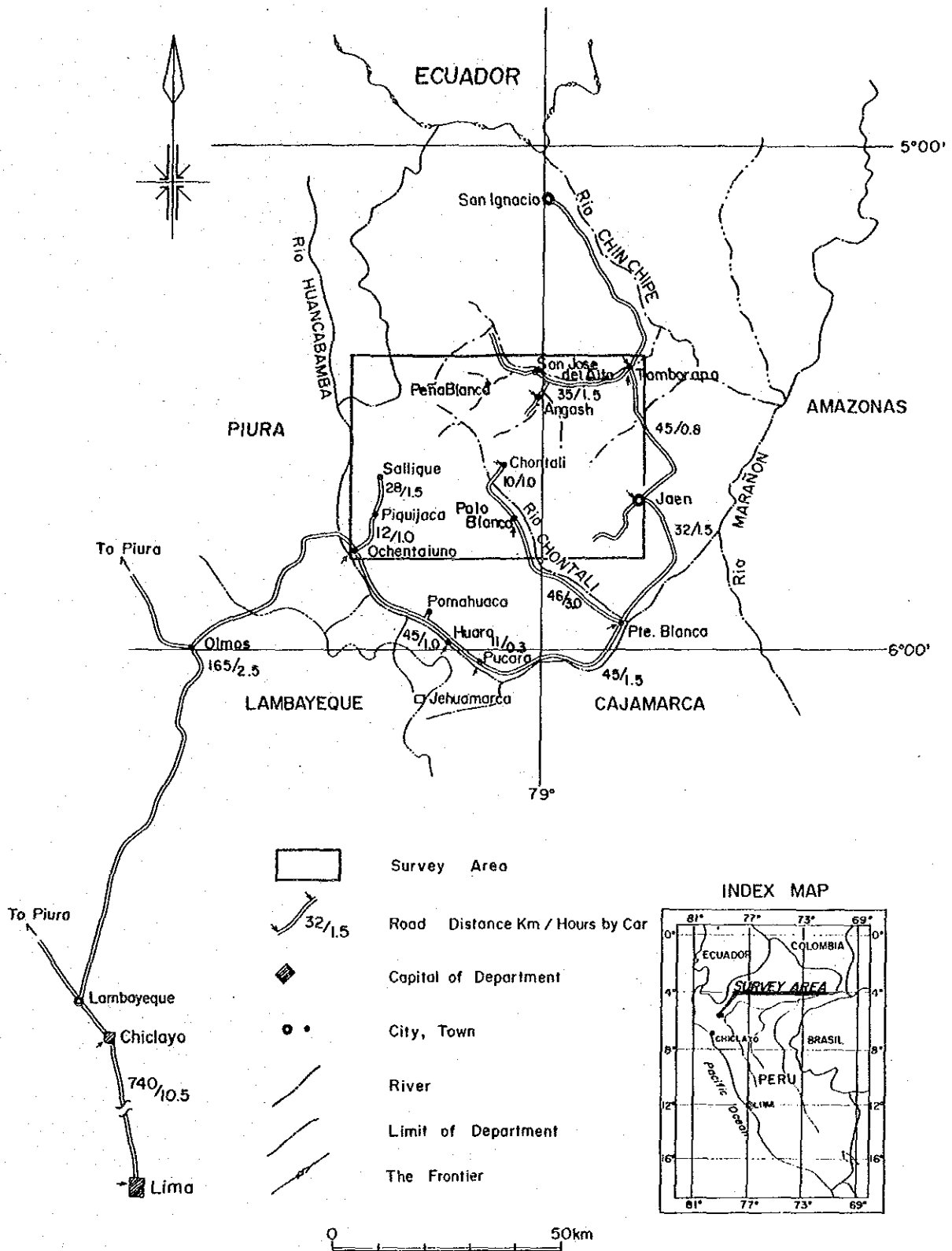


Fig.1-1 (1) Location and Accessibility of the Survey Area

SUMMARY

This report summarizes the third year results of the surveys conducted in the Pachapiriana area, Peru. The surveys aimed to reveal potentiality of an existence of useful mineral resources in the area through clarification of geological setting in the area. The field survey was carried out from July to November, 1990.

The third year survey included drilling survey (16 holes, total length 2334.06m), geophysical survey (gravity survey, 33 km², 305 points) and detailed geological survey (2.5 km²) combined with geochemical survey (100 rock samples).

The drilling survey was conducted in Chontali (6 holes, total length 1332.51m) and Jehuamarca (10 holes, total length 1001.55m) in order to verify the expected mineralization conditions in the deep underground for large-scaled quartz veins and for silicified breccia and quartz zone, respectively. Geophysical survey was performed in Chontali to clarify the feature of gravity basement, which has been inferred to be closely connected with mineralization. Detailed geological survey was conducted in Jehuamarca to clarify the mode of occurrence of silicified breccia and to get the geological informations assisting the interpretation of drilling data.

Through the gravity prospecting it is clarified that the gravity basement has higher density of 2.8g/cm³, and three higher density zones were extracted above the gravity basement. It has also been clarified that drilling cores from northern most high density zone have undergone distinct carbonatization rich in Mn, Fe and Mg and it makes the density higher. Basement granitic rocks may also undergo regional carbonatization to make the density higher. In this case, the density can be as high as 2.84g/cm³.

As a result of the drilling survey, it has been clarified that quartz veins could tend to plunge. If it is the case, the mineralized zones could also plunge.

The analyzed results by homogenization temperature for quartz veins ranged from 102° to 194° C, and rather lower values are predominant. It is inferred that a zone most adequate for gold mineralization can exist deeper than the depth of altitude 1700m, until which this year survey has reached.

It can be inferred that the mineralization in Jehuamarca was progressed at first as argillization under neutral to alkaline environment, then as acidic mineralization, by fluids ascended through the NE-SW to NW-SE subsidiary fault-fissure system branched from regional fault systems and/or through the bedding

boundary.

Silicified breccia and quartz vein, which have been expected to associate gold-silver mineralization and auriferous base metal mineralization respectively, are lower graded than expected and discontinuous, therefore it must be concluded that there is a small possibility that they develop to a large scale high-grade ore body.

For the fourth year survey, it is necessary to conduct drilling survey in Chontali to confirm the plunge of quartz veins as well as mineralization zones, and also to be carried out detailed geological survey combining with detailed mapping and systematic sampling of quartz veins in the quartz vein distributed zone.

PART I GENERAL REMARKS

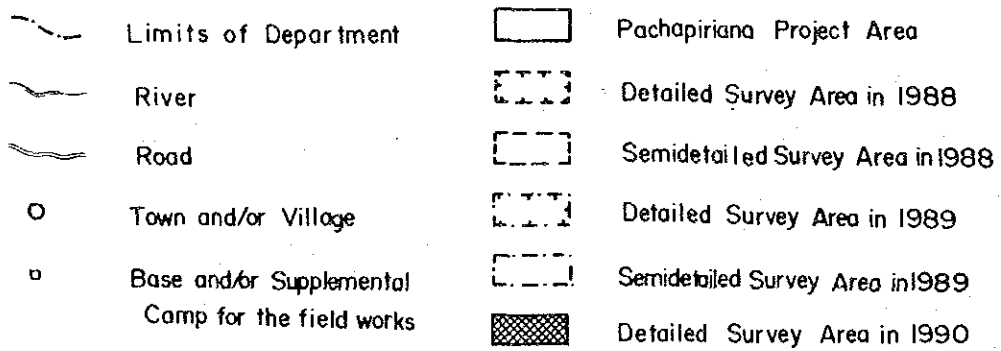
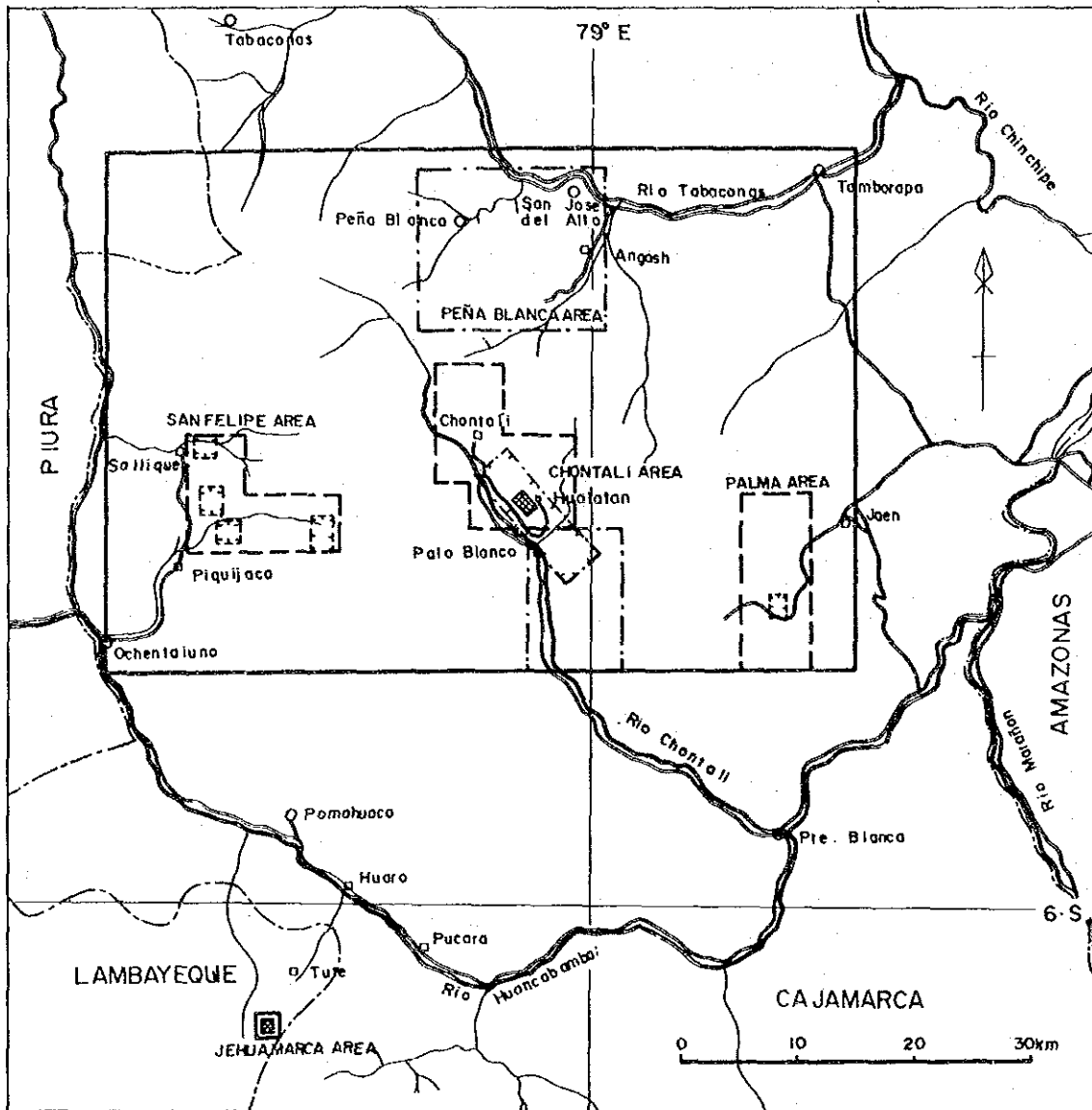


Fig. I-1 (2) Location of the Survey Area

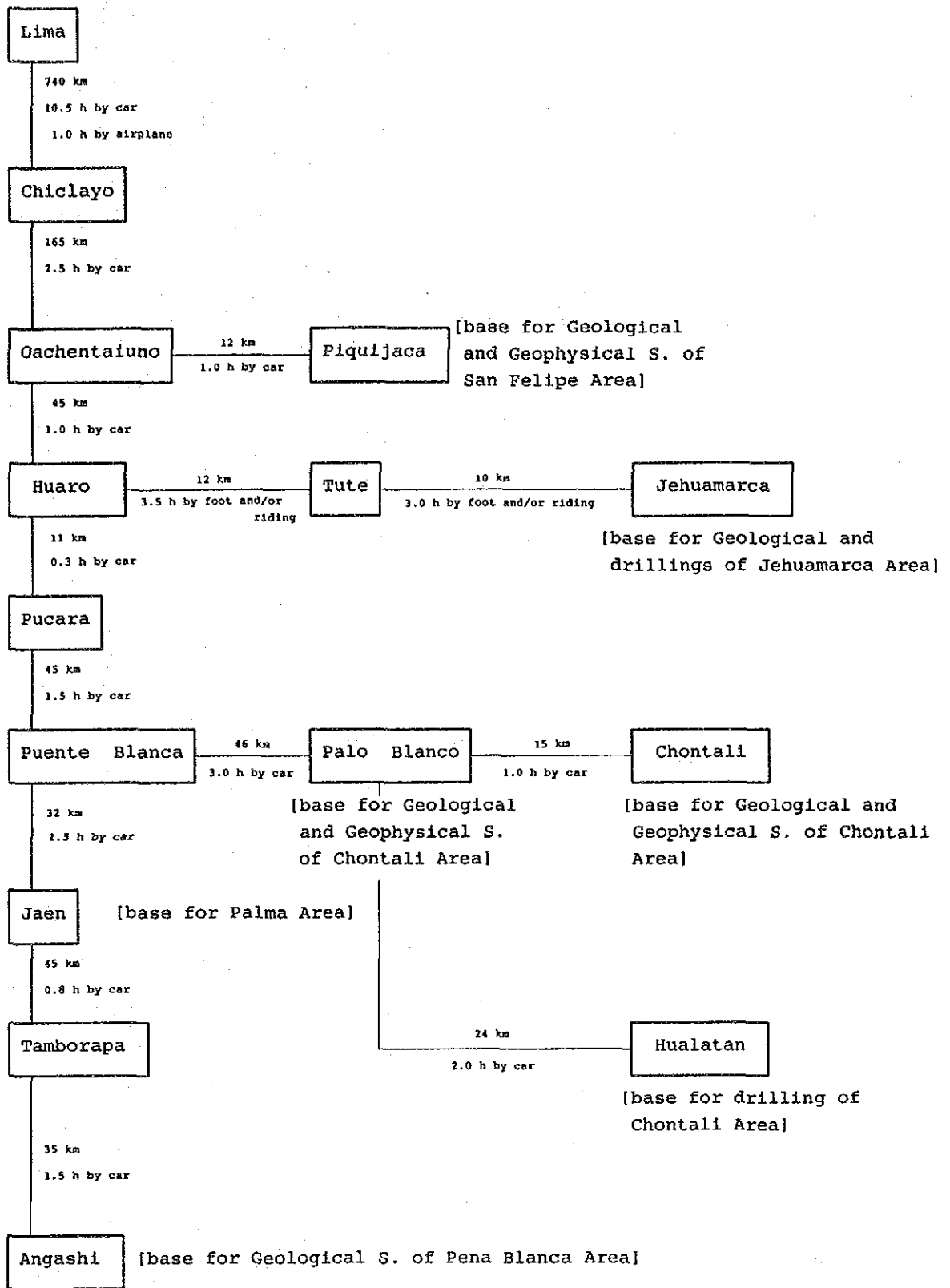


Fig. I-2 Summarized Accessibility of the Survey Area

CHAPTER 1 INTRODUCTION

1-1 Antecedents of the Survey

The survey area is situated in a part of the region for which a geochemical survey using stream sediments was carried out under the Northern Geochemical Project (Proyecto Geoquímico del Norte) sponsored by the U.K. The detailed survey for the extracted geochemical anomalous zones was realized partially by INGEMMET (Instituto Geológico Minero y Metalúrgico) itself and partially by German and French organizations. However, the major part has remained pending due to shortage of funds.

Under these circumstances, INGEMMET requested, through the Ministry of Foreign Affairs of the Republic of Peru, a technical cooperation from the Japanese Government for the follow-up survey in March 1988. In August 1988, a delegation for the preliminary survey and agreement negotiations for this purpose was organized among the Ministry of International Trade and Industry (MITI), Japan International Cooperation Agency (JICA) and Metal Mining Agency of Japan (MMAJ), and sent to Peru. On August 15, 1988, the scope of work to the Pachapiriana area Project was signed between the parties.

According to the scope of work concluded among INGEMMET, JICA and MMAJ, the survey encompasses an area of 2,820 km².

The first year survey included a semi-detailed geological survey which was conducted over a total area of 300 km² in three regions among the geochemical anomalous zones assessed prospective by INGEMMET, combined with the LANDSAT image analysis of entire survey area. An additional detailed geological survey was also conducted over a total area of 25 km², in five regions (21 km²) extracted from semi-detailed survey area and one region (4 km²) extracted by INGEMMET. Geophysical survey using CSAMT method was implemented over 25 km² in two regions. During the second year survey, following the recommendation of the first year survey, detailed geological survey (42 km²), semi-detailed survey (80 km²) and geophysical survey using CSAMT method (35 km²) were conducted in Chontali area. Drilling survey was performed at three sites and total hole length reached 816.25 m in Jehuamarca. Semi-detailed geological survey (220 km²) was conducted in Pena Blanca area.

1-2 Conclusion and Recommendation of the Second Year Survey

1-2-1 Conclusion of the second year survey

The conclusion of the second year survey is summarized as follows:

1) This survey area consists of rocks from Precambrian to Cenozoic.

2) Mineralized alteration occurs in Mesozoic Leche Formation and Ocotun Volcanics and Cenozoic Porculla Volcanics.

3) The mineralized alteration occurs through the NE-SW trending fault systems and its subsidiary NW-SE trending fissure systems, relating to the skarnization and the epithermal mineralization.

4) The skarnization zones suggest the existence of auriferous base metal dissemination type ore deposits and epithermal mineralization zones suggest the existence of epithermal gold and silver vein type and epithermal auriferous base metal vein type ore deposits.

5) Geophysical survey implemented in the Hualatan west in Chontali area, where a high possibility of an existence of epithermal gold and silver vein type has been verified, revealed that the alteration zone was characterized by low resistivity zones and that the silicified and silicified-argillized zones with closely developed quartz veins was extracted as high resistivity within the low resistivity zone.

6) The high resistivity zone continued toward deeper underground as far as the highest part and overlapped to the part part of large-scaled quartz veins within the area with closely developed quartz veins extracted in Hualatan west.

7) Based upon geological setting and the analyzed results by homogenization temperature for quartz veins, the highest resistivity zone is inferred to be connected with the granitic intrusion feature.

8) Average width and length of six quartz veins in the area with large-scaled quartz veins are 3.04m and 80m, respectively. The average grade of veins was 2.54g/ton Au, and 13.99g/ton Ag. The analyzed results by homogenization temperature for the large-scaled quartz veins was lower than 150° C.

9) In Jehuamarca area, it is revealed that the silicified zone is ubiquitously associated with mineralization of gold, silver, copper, lead and zinc, and that the zone can be characterized by a mushroomed structure as interpreted.

10) A layered ore body (quartz zone) of high grade gold, silver, copper, lead and zinc was found in the silicified zone. An existence of high grade gold and silver mineralization zone was confirmed in silicified breccia widely distributed at the surface.

1-2-2 Recommendations of the second year survey

The following surveys are proposed for the third year survey based on the results obtained in the second year:

1) Jehuamarca area

- (1) Drilling survey for silicified zone with high grade layered quartz zone and for silicified breccia zone.
- (2) More detailed geological survey in the area where the drilling survey will be conducted (with a scale of 1/2000, for example).

2) Chontali area

(1) Drilling survey for Hualatan west zone where a high possibility of an existence of high grade gold deposits has been verified.

(2) More detailed geological survey in the area where the drilling survey will be conducted (with a scale of 1/2,000, for example).

(3) Geophysical survey in the area including Hualatan west to clarify the geological structure of basement rocks (gravity prospecting, for example).

3) Tuna area

(1) Semi-detailed geological survey for the geochemical anomalous zones extracted by INGEMMET.

4) Pena Blanca area

(1) Detailed geological survey for mineralization zone extracted in Oyotun Volcanics.

(2) Geophysical prospecting for the mineralization zone (by the CSAMT method, for example).

1-3 Outline of the Third Year Survey

1-3-1 Area and Purpose of the second year survey

The third year survey was conducted according to priority of recommendations of the second year.

1) Jehuamarca area

Drilling survey was performed at ten sites and total hole length reached 1000m. The purpose of the drilling was to verify the mineralized conditions in underground silicified zone and silicified breccia widely distributed at the surface, which have been confirmed to contain a large quantity of sulfide minerals during the second year phase (recommendation 1-1 of the second year).

The propose of drilling at each site is as follows:

MJPJ-4,5,6,7 and 12; to verify the extension of gold and silver mineralization in silicified breccia extracted at MJPJ-3 and to verify the mineralized conditions in deeply underground silicified zone

MJPJ-8,9,10 and 11; to verify the underground extension of the silicified veins extracted at MJPJ-1 and -2 and to verify the mineralized conditions of deeply underground silicified zone

MJPJ-13; to verify the extension and the mineralized conditions of the silicified breccia associated with a fault extracted at MJPJ-3

In order to assist the drilling survey, detailed geological surface mapping combined with geochemical survey was carried out over a total area of 25km², using the route map on the scale of 1/2,000 (recommendation 1-2 of the second year).

2) Chontali area

Drilling survey was performed at six holes and total hole length reached 1332.51m in Hualatan west, where a high possibility of an existence of high grade gold deposits has been extracted in quartz veins (recommendation 2-1 of the second year). The purpose of the drilling was to verify the mineralized conditions in the deep underground.

In order to verify the change of mineralized conditions and mineralization temperature in the deep underground, the survey was conducted by vertically fan-shaped method, in which two holes were drilled at each of three sites.

As the rise of high resistivity basement overlap with the distribution of quartz veins in the alteration zones, it is inferred that the basement structure and mineralization are connected with each other. Therefore, gravity prospecting was performed at 305 points to clarify the geological structure of basement rocks (recommendation 2-3 of the second year).

1-3-2 Survey procedure

The procedure of each survey will be outlined as follows.

1) Detailed geological survey

Detailed geological survey was conducted only in Jehuamarca area this year. A topographical map on the scale of 1/2,500 measured by INGEMMET was used as the base map for the survey. The survey was carried out along measuring lines, which were drawn using string measures and pocketcompasses with a scale of 1/2,000. Measuring lines were closed with each other, except for in some part of outer margin of the survey area. The revision of error of closure was made in terms of horizontal distance. The altitude was measured based on the that of altitude of 3230.0m at triangulation station J-2. The revision of error of closure was made in terms of vertical distance.

Trench survey was also performed to confirm the mode of occurrence of silicified breccia and to draw up a trench map on the scale of 1/100. Route maps on the scale of 1/2,000 were compiled into a geological map on the scale of 1/2,500.

2) Geochemical survey

Rock samples for geochemical survey were taken together with geological survey only in Jehuamarca area. Sampling at the outcrop was carried out as a rule every 100m along the measuring line for detailed geological survey. Sampling density was heightened in the silicified and silicified breccia zones.

3) Geophysical survey

Gravity prospecting was performed in Chontali area using LaCoste gravimeter. Measuring points were set on the measuring line network, which covered whole survey area. The survey was carried out as a rule every 100m in the central part and every 200 to 300m in other parts. Total prospecting points is 305.

The gravity value at standard station was confirmed by the comparison with that at existing gravity station, and the accuracy of measurement was less than 0.2 mgal for closing error.

The altitude at each measuring point was determined by leveling using automatic level of Sokki-sha. The accuracy of measurement was less than $200\sqrt{D}$ (mm) for closing distance D km. If the specification of the measuring point is difficult, stadia measurement and/or distance measurement using esron tape were also applied to make the specification accurate.

The measured gravity values for each point were reduced for such factors as tide, topography, latitude and altitude (Bouguer). Isogravitational map for most adequate assumed density was made using the correlation between gravity anomaly and topographic feature, the results of rock density measurement and G-H correlation method.

Based on the isogravitational map, using Filter analysis and two dimensional analyses, the results of gravity prospecting was indicated on plane figure and cross section, each of which were on the scale of 1/10,000.

4) Drilling survey

Drilling was performed in Jehuamarca and Chontali areas taking the local drilling company GEOTEC, S.A. into employment.

Jehuamarca area

As no roads were passable for motorcars, drilling rig was transported by a helicopter chartered from the Third Peruvian Air Force. The base camp was set up on the summit of Mt. Jehuamarca. The supply bases were set up in Pucara, Huaro and Tute to replenish mending parts, fuel oil, mud, cement and food. Due to the steep configuration, it took two days on outward way and one to two days on homeward to transport the materials from Huaro to Jehuamarca.

Chontali area

The base camp was set up at Hualatan to replenish mending parts, fuel oil, mud, cement and food. Two transit bases were set up at the junction to the national road in Puente Blanco and at the edge of the bridge with a load limitation in Pena Blanca.

5) Quality of the survey

The survey of this year is summarized as follow:

Quality of the Survey							
	geological and geochemical survey		geochemical samples	geophysical survey		drilling survey	
	area km ²	route length km		area km ²	points	hole No.	hole length m
Jehuamarca	2.5	22.176	100			10	1,001.55
Chontali				33	30	6	1.332.51
total	2.5	22.176	100	33	30	16	2.334.06

The rock samples taken for laboratory test are summarized as follows:

Quality of geochemical samples						
	ore analysis	fluid inclusion	X-ray diffraction	thin section	polished section	density
A	12		23	5	2	
B	153		5	4	5	
C						22
D	162	12	20	16	15	

- A: detailed geological survey in Jehuamarca
- B: drilling survey in Jehuamarca
- C: gravity prospecting in Chontali
- D: drilling survey in Chontali

1-3-3 Organization of the survey group and period of the survey

The representatives from Japanese government for the third year survey and agreement negotiation were dispatched to Peru during the period from July 3 to 6, 1990. The delegation members and their counterparts in Peru are shown below:

From Japan:
Mr. Hideya METSUGI, Metal Mining Agency of Japan

CHAPTER 2 GEOGRAPHY OF THE SURVEY AREA

2-1 Topography and Drainage System

The third year survey was conducted in the central part of the survey area as shown in Fig.I-1(2).

In Chontali area, the Chontali (called as the Huallabamba or the Chunchuca, on different topographic maps) runs along the west boundary southward in the direction of NW-SE. Each tributary tends to meet nearly at right angles to the Chontali, namely they are arranged in the direction of NE-SW.

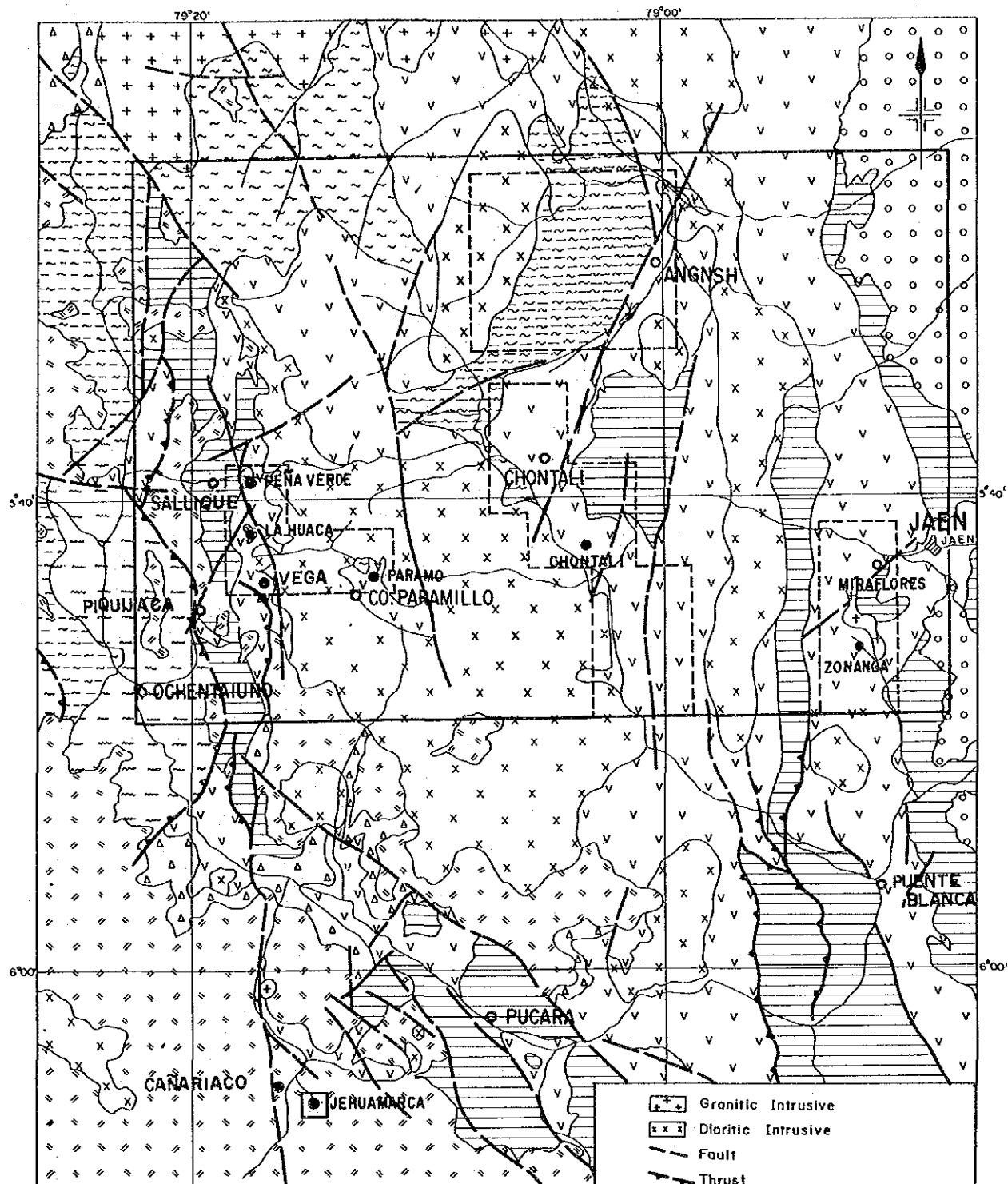
In Jehuamarca area, the semi-basin opened northwestward develops and the drainage system is dendritic, the main river of which runs northwestward.

Both of the areas are topographically so steep. In Chontali area, the elevation is 1650m between the Chontali(1050m above the sea level) and the highest peak(2700m). In Jehuamarca area, though the area is narrow, the elevation is as high as 320m between the river-side in the central west (3085m) and the highest peak in the central north (3405m). Cliffs are so steep with the average slope angle more than 60° in the north and east that climate is locally changed.

2-2 Climate and Vegetation

As reported last year, vegetation in the survey area show a particularly remarkable variation due to the altitude difference. Another critical factor for the variation is whether the land is reclaimed or not. The area belongs essentially to tropical to subtropical rainforest zones characterized by thick virgin forests with trees of 10 to 15m high. In the progress of disafforestation, the desert has been expanded but the irrigated area are preserved as agricultural lands but non-agricultural lands become dry shrubbery zones.

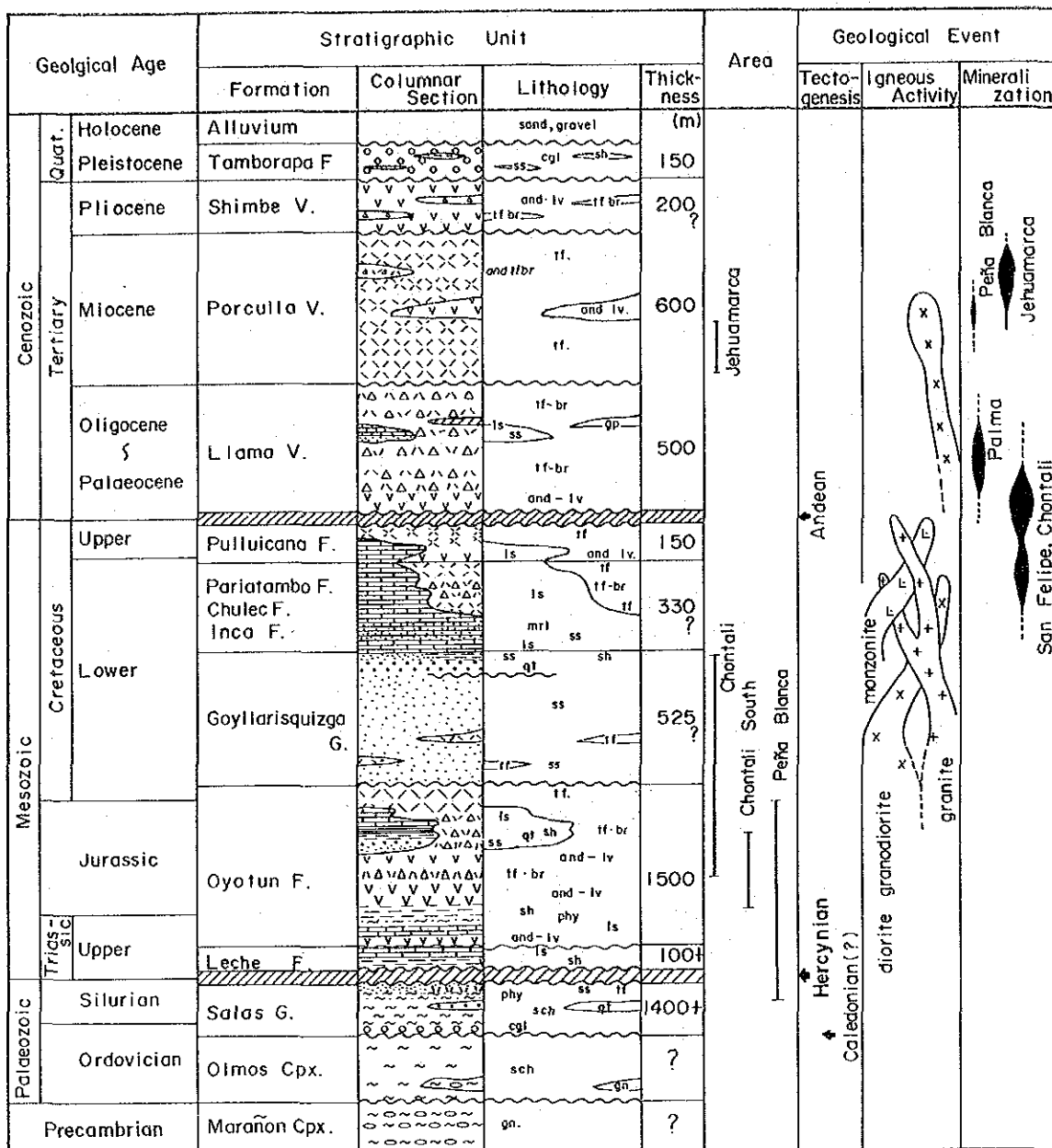
In Chontali, whole survey area has been reclaimed to be used as agricultural or pasture lands. In Jehuamarca, whole survey area has not yet been reclaimed due to the cool climate. It is covered with paja (needle-like grass) and is used as natural pasture land. Northern, eastern and almost of southern parts are covered with virgin forest, thus the survey is very difficult, coupled with the steep topography. Although climate in the survey area seems to show remarkable local variation, it is difficult to systematize the variation because meteorological observation stations are few and meteorological data are poor. Temperature shows a remarkable variation due to the altitude. The average values decrease as the altitude becomes higher. The average temperature variation for each month is so small that it can be said the seasonal variation of temperature is slight. However, it is inferred that the diurnal variation is very large, as the difference between maximum and minimum temperatures for



Quaternary	Tamborapa Formation		Shale, sandstone, conglomerate
Tertiary	Porculla Volcanics		Andesite, tuff, tuff breccia
	Llama Volcanics		Tuff breccia, sandstone, limestone, gypsum
Cretaceous	Goyllarisquiza Group		Quartzite, shale, sandstone, limestone
Jurassic Triassic	Oyotun Volcanics		Andesite, tuff, tuff breccia, shale, limestone
Silurian Ordovician	Salas Group		Phyllite, schist, quartzite, conglomerate
Cambrian	Olmos Complex		Schist, gneiss,
Proterozoic	Marañón Complex		Gneiss

Fig. 1 - 3 Generalized Geological Map of The Survey Area

modified from Wilson (1984), Reyes et al (1987) and Davila et al (unpubl)



Abbreviations.

and	andesite	gn	gneiss	md	mudstone	sch	schist
acd	acidic	gp	gypsum	mrl	marl	sh	shale
br	breccia	ls	limestone	phy	phyllite	ss	sandstone
cgl	conglomerate	lv	lava	qt	quartzite	tf	tuff
F.	Formation	V.	Volcanics	G.	Group.	Cpx.	Complex

Fig. I-4 Generalized Stratigraphic Column of the Survey Area

each month is more than 10° C.

Relative humidity tends to be higher as the altitude becomes high in contrast to the case of temperature. Judge from the average humidity for each month, the variation coincides with that of average temperature, independently to dry or rainy period.

The precipitation is not dependent on the altitude but fairly on the presence of virgin forest in the surrounding.

Annual variation of precipitation is not so remarkable and there is not a clear distinction between the rainy and dry periods. If a month belonging to the rainy period is defined as with more than 100mm precipitation, the rainy period covers December to March and the dry one June to November. Among the periods, January to April and July to September are relatively much and less precipitated, respectively.

In Jehuamarca, no meteorological data are available. The whole survey area is always covered with nimbus grown by an ascending current to characterize a typical local climate. The current is formed when the atmosphere with high humidity supplied from northern and eastern parts covered with virgin forest collides with steep cliffs in northern and eastern parts.

CHAPTER 3 GENERAL GEOLOGY

The survey area is situated in a southernmost of the tectonically disturbed zone, so called Huancabamba deflexion zone. This causes a great variation of rock facies of each geological unit among the former surveys. In addition most of the survey area is uncivilized and the accessed of the survey routes is not easy, thus bringing some confusion to correlate geological formation and it requires further study.

An geological outline of the area is given below after Wilson(1984), Reyes y Caldas(1987) and Davila et al(unpublished), revised after the results of first and second years geological survey. A geological map and a stratigraphic column are generalized as shown in Figs. I-3 and I-4, respectively.

The survey area consists of metamorphic rocks correlative with Precambrian to Paleozoic, Mesozoic sedimentary and volcanic rocks and Cenozoic volcanic and intrusive rocks.

The metamorphic rocks, consisting of the basement Marañon Complex, Ordovician Olmos Complex and Silurian Salas Group, have such a wide lithofacies as gneiss, schist and phyllite. They are developed in the western half of the survey area.

Mesozoic rocks are the main constituent of the survey area and consist of the following units in ascending order: Leche Formation (mainly calcareous rocks), Tinajones Formation (arenaceous rocks intercalated with tuffaceous rocks), and Inca, Chulec, Pariatambo and Pulluicana Formations (mainly calcareous rocks).

Cenozoic rocks composed mainly of volcanic rocks which in ascending order are Llama, Porculla and Shimbe Volcanics, distributed in western and southwestern parts of the survey area. Tamborapa Formation consists of conglomerate, with loose consolidation, being correlative with the Quaternary sediments. This Formation occurs at the eastern flange of the survey area.

Intrusive rocks consist of gabbros, diorites and granites. Generally, gabbros and diorites are older than granites which are intruded even Porculla Volcanics.

The absolute ages determined using K/Ar method are 119 ± 6 million years for quartz diorite, 106 ± 5 million years for quartz monzonite, 82.5 ± 4 million years for granodiorite, 78 ± 3.9 million years for monzonisyenite and 47.6 ± 2.4 for adamellite. The intrusive trends are tend to be NW-SE and N-S, reflecting the geological structure.

Geological structure of the survey area is characterized by its situation of which located at the south flange of a distorted zone of general Andean Trend. This distorted zone, so called the Huancabamba Deflection Zone, corresponds to the area at which the general NNW-SSE direction, the basic characteristic of the Andes, changes direction to the NE-SW trending of the Colombia-Venezuela area. This deflection zone is assumed to have been formed during the Mesozoic tectogenetic movement.

Two combined fault systems are observed in the survey area.

One is E-W with NE-SW trending caused by an east-west lateral compression, and another is N-S with NNW-SSE trending by northwest-southeast one. Both these systems reflect the tectonic movement at the time when the Huancabamba Deflection Zone was formed.

CHAPTER 4 SURVEY RESULTS, COMPREHENSIVE ANALYSIS

4-1 Geological Structure, and Characteristics and Controlling Factors of the Mineralization

This survey area is regionally located in the Huancabamba Deflection Zone, that is, the area belongs to a distorted zone of the general Andean trend in NW-SE changes to NE-SW trending.

1) Chontali area

It was concluded by last year survey that alteration and quartz zones occur on the secondary branched NW-SE fissure zone developed between the regional NE-SW fissure systems. As a result of microscopic observations for drilling cores taken through this year survey, it is concluded that the tectonic movement has continued even after the formation of quartz vein, because quartz grains in quartz vein and in fracture zone extended from the quartz vein commonly show undulatory extinction. Moreover, as fracture zone without quartz vein is in large scale and continuous, and a large-scaled quartz vein is pinched out (MJPJ-2) or branched (MJPJ-4) in fracture zone, it is assumed that quartz vein develops in fracture zone controlled by the structure of fracture zone (unidentified up to now). In other words, quartz vein could tend to plunge, and if it is the case, the mineralization zone could also plunge.

As ore minerals containing such valuable metals as gold, silver, zinc, copper, lead and so on are closely associated with each other, the mineralization environment is inferred to be xenothermal. It is worthy of note that the alteration is characterized by the occurrence of carbonate minerals suggesting the neutral to alkaline environment and that the minerals are composed mainly of such heavy metals as Fe, Mn, Mg and so on.

2) Jehuamarca area

Though distinct fissure systems trend NE-SW and NW-SE, the displacement along the systems are a few to ten and a few meters. Additionally, the fissure systems are other discontinuous. Therefore, they are concluded to be the secondary or third systems branched from major tectonic systems. Along the fissure systems, it is schematically assumed that southern and eastern sides have been displaced downward.

It can be inferred that the mineralization in Jehuamarca was commonly characterized by argillization under neutral to alkaline environment, then overlapped acidic mineralization by fluids ascended through the above-mentioned fissure systems and/or through the bedding boundary. This mineralization process could make the mineralization zone to distribute as stratiform.

4-2 Potentiality of an Existence of Ore Deposits

The survey area contains numerous geochemical anomalous zones with using the stream sediments which were previously sampled by INGEMMET in the "Proyecto Geoquimico del Norte" and the "Proyecto Integral Chinchipe". Semi-detailed geological survey has been continued to implement up to last year to find out to what origin these anomalies were attributed. As a result, obvious mineralized alteration was verified in the backland of the rivers where geochemical anomaly is marked. Therefore, we can conclude that the geochemical anomalies extracted by INGEMMET suggest an existence of mineralized indications.

While no economical ore deposits have been found as yet, the follow-up study of the aforementioned "Proyectos" verified that the existence of La Granja ore deposits and Canariaco ore deposits. In addition, it is reported that a stratiform gold deposit and an epithermal gold deposit have been found in the northern part of this survey area by the "Proyecto Integral Chinchipe: Cordillera del Condor" which is currently under way. It is certain that the area contains promising mineralized area.

Detailed geological survey, which was conducted last year for the Chontali alteration zone extracted in the first year survey, has confirmed the existence of predominant silicified alteration zone with abundant quartz veins and veinlets. Moreover, the geophysical survey conducted last year confirmed a three-dimensional distribution of mineralized alteration zones with quartz veins. Drilling survey performed this year has confirmed the underground fracture zone in large scale (yet unidentified on the surface) and native gold is extracted from the quartz vein in the zone, therefore it becomes more certain that the area contains promising mineralized area.

Drilling and trench surveys performed this year for Jehuamarca alteration zone, where three-dimensional distribution of mineralized alteration zone had been assumed up to last year, have confirmed the frequent existence of distinct mineralization zone, though in small scale. As affairs now stand, the whole average grade of the mineralization zones is relatively low, there is a small possibility that it develop to a large scale ore body, but it still has a potential for resources in the future or a small-scaled mining.

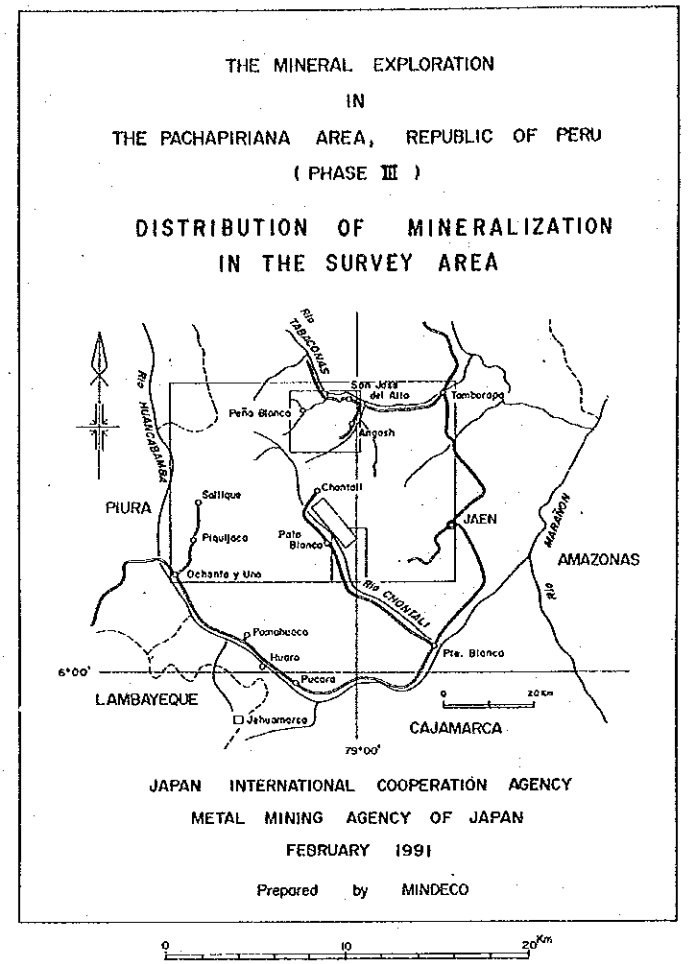
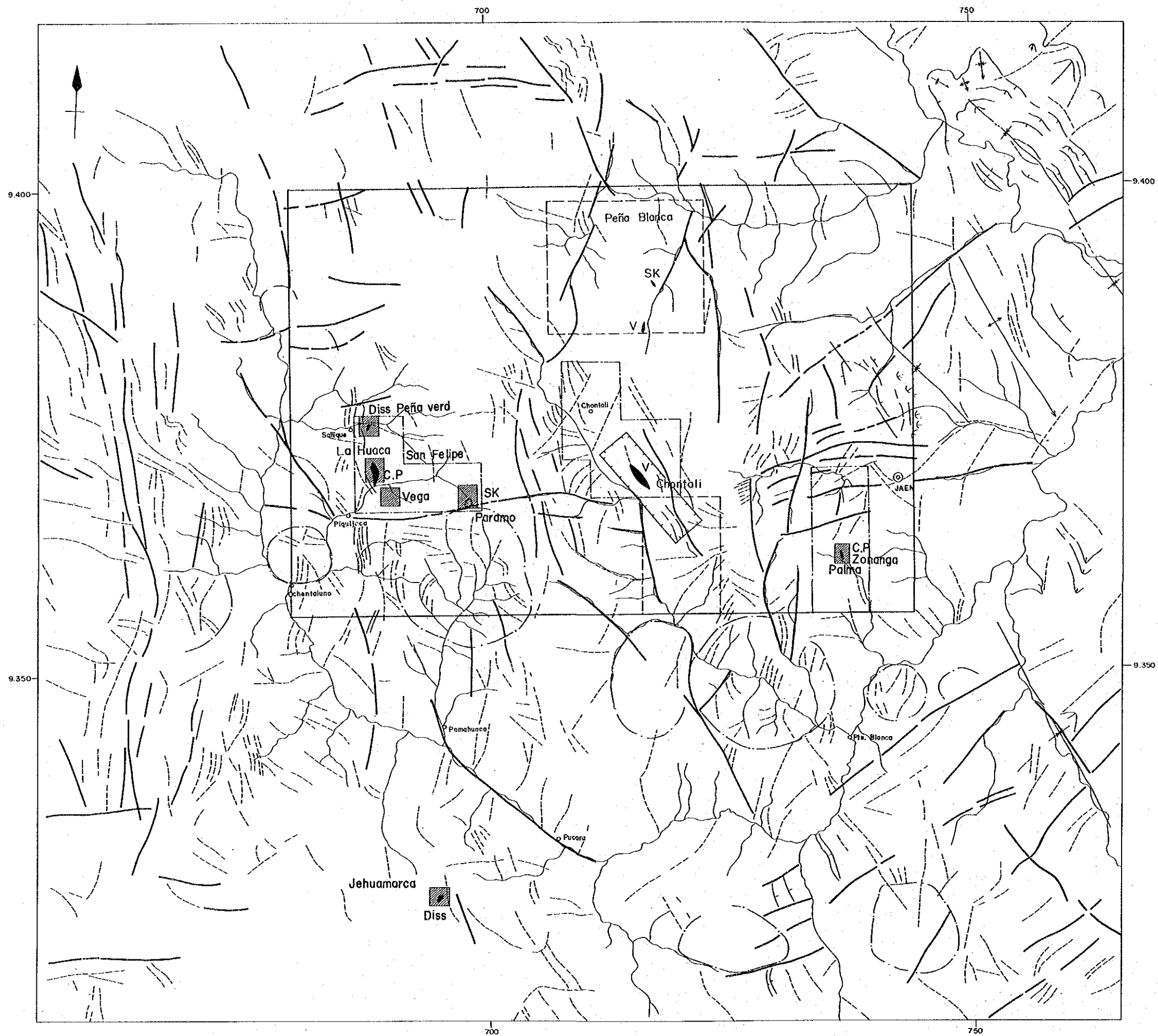
4-3 Relation between Geochemical Anomaly and Mineralization

Geochemical anomalies obtained up to last year was assumed to be classified into driving from mineralized alteration and indicating horizons. The latter is inferred to correspond to the anomalous values found by geochemical survey of the first year, whose distributions were detected in the Salas Group, Chontali. It is clarified, however, by geochemical survey conducted in Jehuamarca this year that zinc anomaly exists along the andesitic sheet in the southwestern part, suggesting the close connection

of geochemical anomaly with a specific rock. In this connection, andesite itself contains zinc as high as 5045ppm (two specimens, arithmetic mean).

Geochemical anomalies obtained this year tend to be distributed overlapping to or around the silicified breccia and fissures, except for a part of zinc anomaly mentioned above.

Due to the weathering, silicified breccia tends to contain no sulfide minerals. Through the preparation of the drilling site of MJPJ-5, however, a sulfide ore body with a large quantity of sphalerite associated with tetrahedrite at the base of silicified breccia has been extracted. Thus, gold and silver mineralization zone now extracted is originally derived from auri-argentiferous base metal mineralization zone. It is concluded, therefore, that geochemical anomaly in this area is closely connected with original mineralization. Regarding the geochemical anomalies distribution of each element, gold anomaly tends to be distributed in the central part and silver, lead and silver anomalies surround it in order outward, to reflect the thermal gradient during the mineralization.



LEGEND

- MAJOR LINEAMENTS
- MINOR LINEAMENTS
- CIRCULAR FEATURE
- BEDDING
- ANTICLINAL AXIS
- SYNCLINAL AXIS
- Pachapiriana Project Area
- Detailed Survey Area in 1988
- Semidetailed Survey Area in 1988
- Detailed Survey Area in 1989
- Semidetailed Survey Area in 1989
- Mineral Indication
- C.P. : Porphyry Copper Type
- Diss : Dissemination of Base Metal Type
- V : Vein Type
- Sk : Skarn Type

Fig. I-5 Distribution of Mineralization in the Survey Area

CHAPTER 5 CONCLUSION AND RECOMMENDATION

5-1 Conclusion

1) Chontali area

It is clarified, through the gravity prospecting that the gravity basement with the density of 2.8g/cm^3 is widely developed underground. The value is rather higher than observed density (2.68g/cm^3) of granitic rocks on the surface which is inferred to constitute the basement. Meanwhile, it has been clarified through this year drilling survey that drilling cores have undergone distinct carbonatization rich in heavy metals, which could not be extracted through the surface survey. The arithmetic mean density of drilling core and the specimen taken from surface is 2.71g/cm^3 and 2.56g/cm^3 respectively, namely the former is 5.9% higher than the latter. If it is assumed that basement granitic rock has also undergone regional carbonatization, its density can be as high as 2.84g/cm^3 . It, therefore, is possible to suppose that the high density basement is composed of carbonatized granitic rocks. As compared with the distribution of high resistivity zone extracted through last year geophysical survey by CSAMT method, the high density basement (gravity basement) is, though showing similar undulation, rather shallower. It is solely due to the lack of control points to regulate the relative depth of gravity basement. Among the high density zones just above the gravity basement, the northernmost one is just situated in the area for drilling survey this year. The area extracted as high density can almost coincide with localized mineralization-alteration zone such as highly carbonatized zone. Drilling survey was performed this year based on the assumption that the enriched mineralization zone on the surface can continue directly under the outcrop. Quartz vein extracted by drilling survey exists in breccia (fracture) zone in which quartz grains show distinct undulatory extinction, the zone having been confirmed to continue even when quartz vein has been pinched out. It is suggested that quartz vein could tend to plunge as it is pinched out or branched within the fracture zone. If quartz vein tends to plunge, it must be interpreted that the enriched mineralization zone could also plunge. Although the analyzed results this year shows that quartz vein is lower grade than expected, native gold grain is confirmed in one specimen by microscopic observation to suggest the possibility of an existence of high grade gold mineralization zone. Moreover, ore minerals containing such metals as silver, copper, zinc and lead are closely associated with each other, thus the mineralization environment is assumed to be xenothermal. Namely, it is possible that the mineralization zone could change into base metal ore deposit deep underground.

The analyzed results by homogenization temperature for quartz veins ranged from 102° to 194°C , having rather lower

values with a mean of 137° C. It is inferred that a zone most adequate for gold mineralization (180° to 230° C) can exist deeper than the depth of altitude 1700m, until which this year survey has reached. The temperature distribution on geological sections show that higher and lower temperature zones develop western and eastern parts of survey area, respectively. It supports the conclusion of last year that in the west part of the survey area there exists the highest center, say heat source of granitic rocks.

2) Jehuamarca area

Based upon the results of detailed geological survey and drilling survey this year, the mineralization model was assumed to be as follows. Along the secondary or third NW-SE and NE-SW fissure systems, which are branched from regional fault system, associated with small displacement and along the bedding boundary, argillization under neutral to alkaline environment has progressed followed by silicification with mineralization under acidic condition. Therefore it is inferred that three types of mineralization (i.e. base metal mineralization with silicification, high grade layered base metal mineralization within quartz zone and gold and silver mineralization within silicified breccia) shown last year are essentially a series of mineralization. Namely gold-silver mineralization in silicified breccia is a residual deposit, which is formed from auri-argentiferous base metal mineralization zone altered by meteoric water. High grade layered base metal mineralization in quartz is a typical base metal mineralization zone formed by silicification.

Silicified breccia occur continuously as a stratiform, but the mineralization zone of gold and silver is localized and their grade seems to change frequently, therefore it must be concluded to be lower grade than expected. Quartz zone expected to associate high-grade base metal mineralization is discontinuous and changes its thickness and grade frequently, therefore there is a small possibility that it develops to a large scale high-grade ore body.

5-2 Recommendation for the Fourth Year Survey

The following surveys are proposed in the order of priority for the fourth year survey based on the results obtained in third year:

1) Chontali area

(1) Drilling survey at more than two holes to confirm the plunge of quartz vein.

(2) More detailed geological survey combining with detailed mapping and systematic sampling of quartz veins in the quartz vein distributed area will be conducted (with a scale of 1/2000, for example).

PART II PARTICULARS

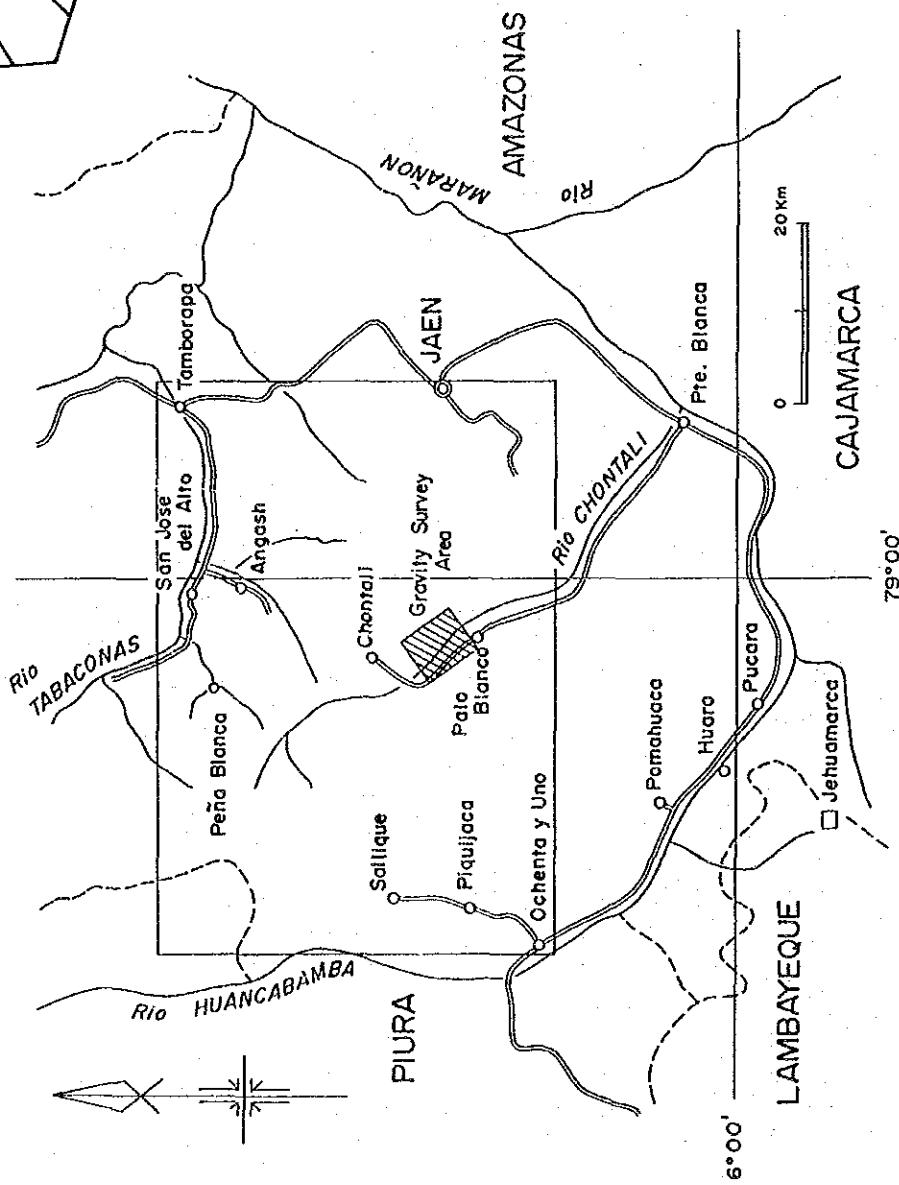
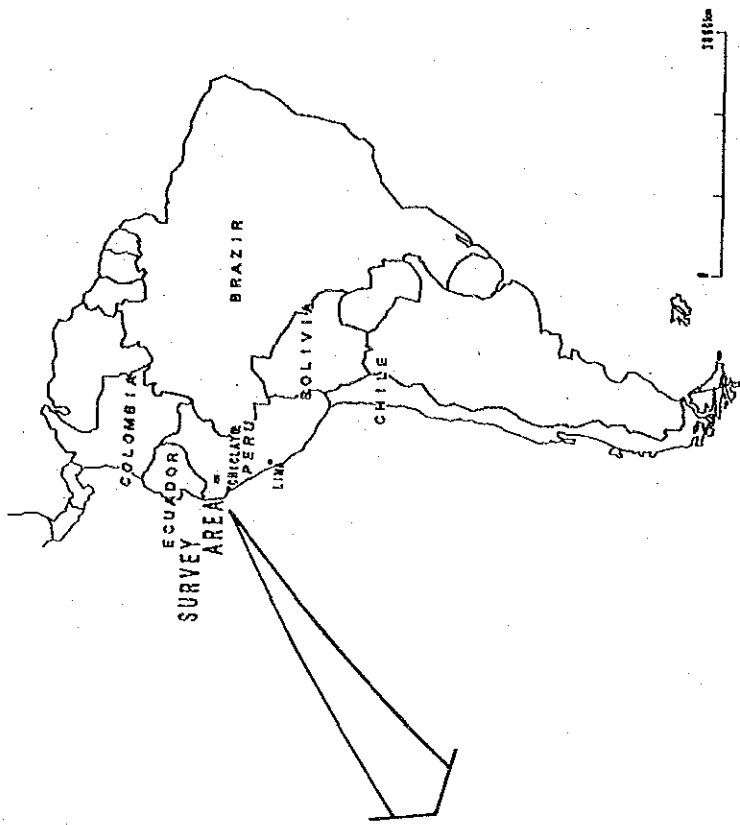
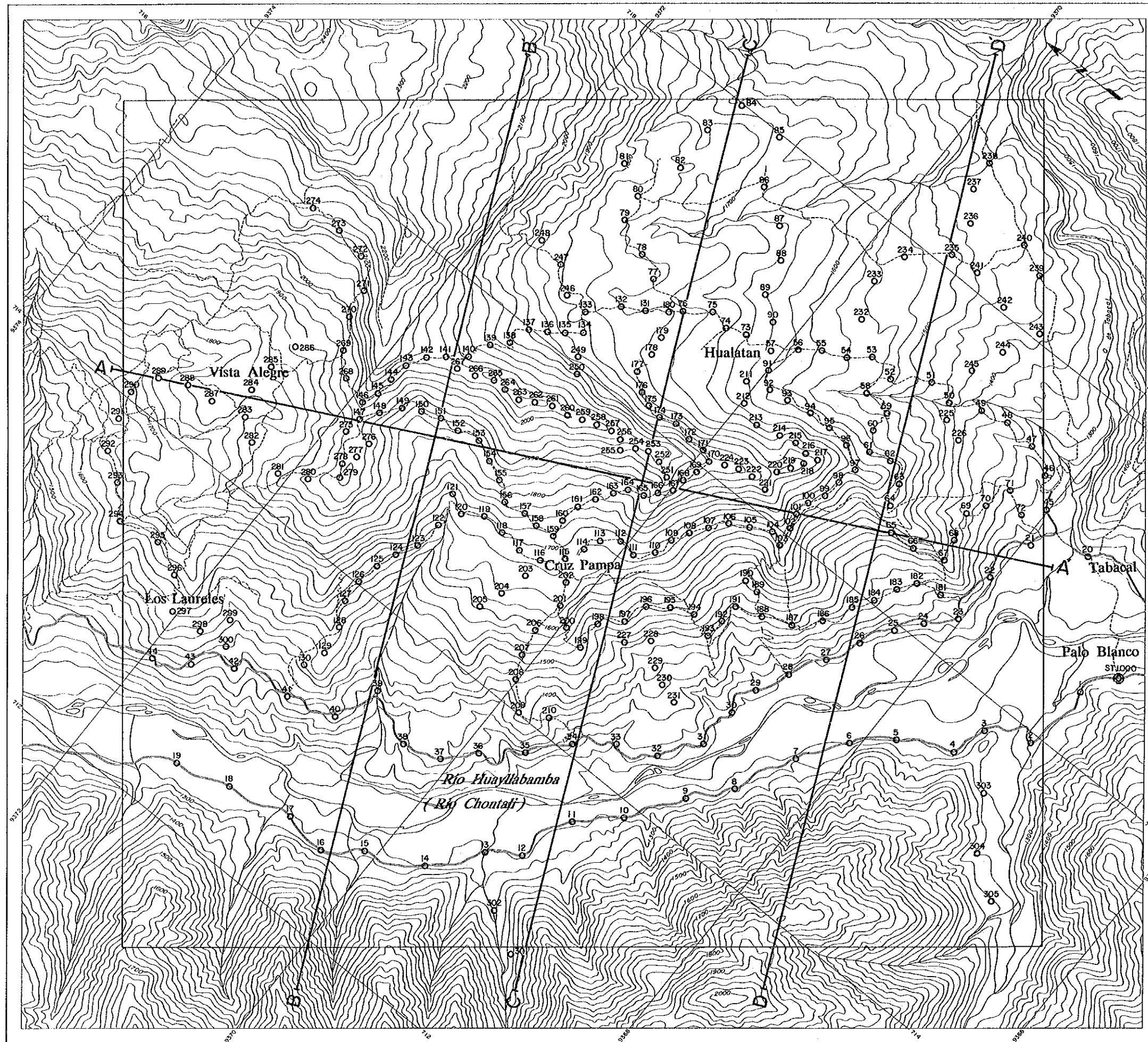


Fig II-1 Gravity Survey Area



LEGEND

- ⊙ Base station
- 305 Station number
- Gravity station
- A-A' Cross section

THE MINERAL EXPLORATION
 IN
 THE PACHAPIRIANA AREA
 REPUBLIC OF PERU
 (PHASE III)

GRAVITY SURVEY

Fig. II-2
 Location of
 Gravity Stations

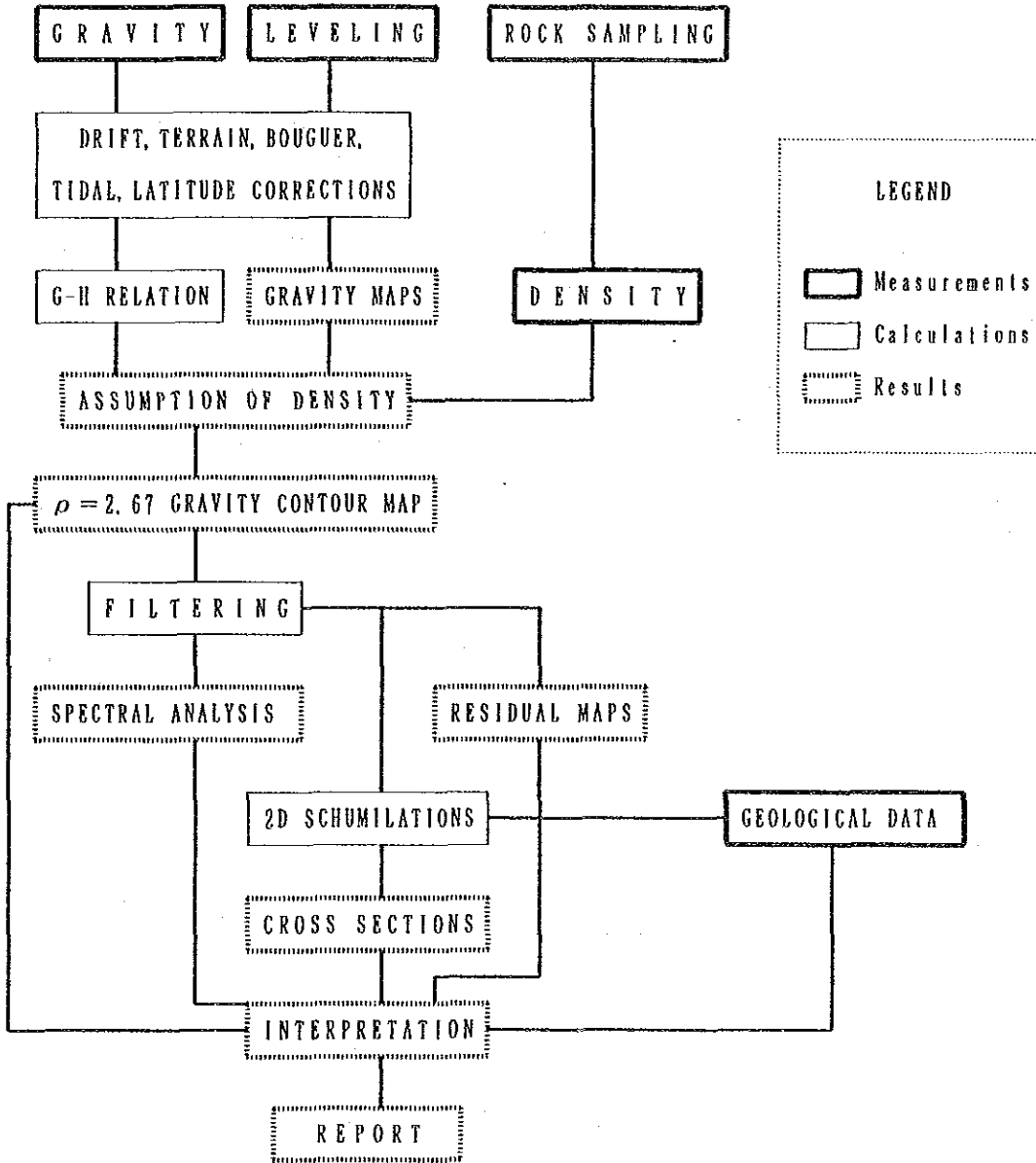
FEBRUARY 1991



CHAPTER 1 CHONTALI AREA

1-1 Geophysical Survey

The procedure followed in this gravity survey is shown schematically as follows:



1-1-1 Gravity stations

This gravity survey area and the location of gravity stations within the survey area are shown in Fig.II-1 and Fig.II-2. Hualatan is located in the center of the area in a geological district of quartz vein occurrence.

Gravity measurements were made at a total of 305 locations with a dense distribution of gravity stations surrounding Hualatan.

1-1-2 Gravity measurement

1) Gravimeter

The instrument employed in this survey was a G-283 Lacoste & Romberg, Inc. gravimeter. The specifications of this device are as follows:

TYPE	La Coste & Romberg. INC Model G Geodetic Gravimeter
No.	283
Operation Range	0~ 7,386.54 mgal
Temperature	51.7°C
Reading Line	2.80
Date of Production	Jan., 1972
Dimensions	14× 15× 20

This gravimeter has a wide operating range and is capable of measuring gravity from values of 0 mgal to more than 7000 mgal. Very precise measurements can be made with this device in that it has an accuracy of +0.01 mgal and an instrument drift rate of only 1 mgal/month. This allows the collection of precise data while requiring only daily closure.

2) Standard Absolute Gravity Value

We utilized a standard absolute gravity value at a base station identified as CQCH-1. The base station is located on the edge of a bridge near Chamaya in southern Jaen. The standard absolute gravity value is taken as 977,853.54 mgal.

A temporal base station, ST.1000, was established in Palo Blanco where the survey crews were housed. Measurements were made twice per day at the temporal base station to establish a standard absolute gravity value of 977,687.179 mgal.

Closure of gravity values measured during the course of this survey was made by the Potsdam system.

Table II-1 Calculations of Gravity Standard Value

Observer : K.KINOSHITA

date of observation station number	time	reading value	x constant (mgal)	height of gravitymeter (m)	H.G. correction (mgal)	tide correction (mgal)	drift correction (mgal)	total correction (mgal)	difference from Base (mgal)	absolute gravity (mgal)
1990.07.27										
ST.1000	9:15	1301.588	1372.134	0.27	0.083	0.069	0.0	1372.286	0.0	977,687.165
1990.07.30										
CQCH-1	12:11	1459.415	1538.550	0.27	0.083	0.066	-0.038	1538.661	+166.375	977,853.54
CQCH-1	12:28	1459.393	1538.527	0.27	0.083	0.062	-0.038	1538.634	+166.348	977,853.54
ST.1000	18:04	1301.705	1372.258	0.27	0.083	-0.014	-0.041	1372.286	0.0	977,687.192

absolute gravity of ST.1000(average): 977,687.179 mgal

1-1-3 Leveling

The direct leveling method was employed for all 305 stations using an Auto level B-2 made by Sokkisha of Japan. Terrain corrections were made by cross section leveling.

An elevation correction value was determined by measuring the elevation of 88 stations relative to the temporal base station by leveling. The elevation of the base station and the leveling stations were then taken from topographic maps and the mean error determined. This shift value (1214.95m) was then added to the elevations measured at gravity stations by leveling.

The accuracy of leveling is expressed as follows:

$$\varepsilon \leq 20 \sqrt{D}$$

where, ε : error of leveling(cm)

D : closure distance(km).

The error of closure is divided among readings in relation to the horizontal distance from the measurement point to the leveling base station.

1-1-4 Corrections and data processing

In order to be most useful in prospecting, gravity data obtained in the field must be corrected for tide, height of instruments, drift, latitude, influence of topography, altitude, free-air, Bouguer, and so on.

The results of these corrections are presented in Table II-3.

1) Tidal correction

Tidal forces result from the attraction of the sun and moon at earth's surface. These vary in direction and intensity with time and place of observation.

Tidal forces due to the sun and moon are calculated by the following formula:

$$\Delta g = -3/2 GM a / r^3 \{3(\sin^2 \delta - 1/3)(\sin^2 \delta - 1/3) + \sin 2\delta \sin 2\phi \cos \theta + \cos^2 \delta \cos^2 \phi \cos 2\theta\} \times 1.2 \text{ (gal)}$$

where, G : gravitational constant = 6.67×10^{-11} ($\text{m}^3 / \text{kg} \cdot \text{sec}^2$)
M : mass of the planets (moon: 7.348×10^{22} kg, sun : 1.9891×10^{30} kg)
a : distance from the center of the earth to the station
= $6378388(0.99832 + 1.6835 \times 10^{-6} \cos 2\phi - 3.5 \times 10^{-6} \cos 4\phi)$ + altitude of the station(m)
r : distance from the center of the earth to the planet
(moon: 3.844×10^8 m, sun : 1.496×10^{11} m)
 ϕ : latitude of the station

δ : declination of the planet
 θ : hour angle of the planet.

2) Drift correction

In the case of spring-balance type gravimeter, drift is caused by creep of the spring material. The influence of the drift is accounted for by assuming that the drift values vary proportionally with time. In this survey, the drift rate is less than 0.2 mgal/day.

3) Terrain correction

A topographic irregularity(hill, knoll, slope, valley, etc.) exerts an attraction directly proportional to its density. The vertical component of this attraction is directed upwards and reduces the observed gravity. Therefore, a term of equal magnitude must be added to the observed gravity.

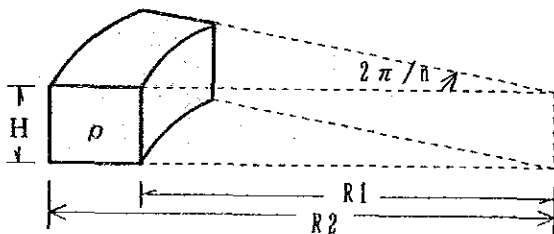
It is necessary to compensate for such effects when topographic features are sufficiently close to an observation point to cause distortions in the observed gravity which are large enough to affect the interpretation of anomalies. For this reason, topography near measurement stations has to be considered in more detail.

The usual procedure in making corrections for such distortions is to estimate the average altitude by computer within each compartment shown in Fig.II-3 using gridded altitude data from topographic maps. The terrain correction is calculated by dividing the area around the station into three groups, far, middle, and near area.

(1) Hammer's method

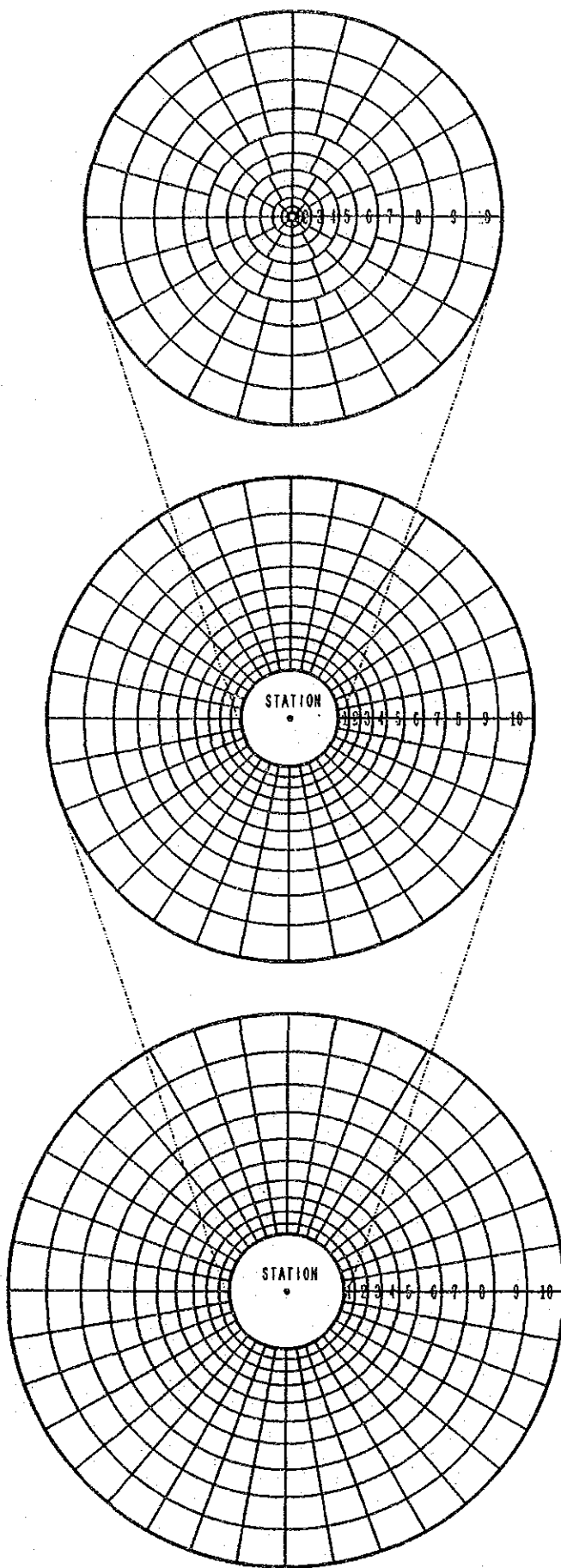
The terrain corrections for far, middle, and near areas are calculated by Hammer's method as shown the following form:

$$\Delta g = 2\pi G \rho / n \{ R_2 - R_1 + (R_1^2 + H^2)^{1/2} - (R_2^2 + H^2)^{1/2} \}$$



where,

- Δg : terrain correction value(mgal)
- G : gravitational constant
- ρ : correction density (g/cm³)
- R_1 : inner radius of compartment(m)
- R_2 : outer radius of compartment(m)
- H : altitude of station(m)



[NEAR]

Data Grid Interval = 100 m

No.	Distance from Station	Number of Block
1	30 ~ 90 ^m	8
2	90 ~ 180	8
3	180 ~ 300	12
4	300 ~ 450	12
5	450 ~ 600	16
6	600 ~ 800	16
7	800 ~ 1,050	24
8	1,050 ~ 1,350	24
9	1,350 ~ 1,650	24
10	1,650 ~ 2,000	24

$\Sigma=168$

[MIDDLE]

Data Grid Interval = 500 m

No.	Distance from Station	Number of Block
1	2.0 ~ 2.4 ^{km}	32
2	2.4 ~ 2.8	32
3	2.8 ~ 3.3	32
4	3.3 ~ 3.9	32
5	3.9 ~ 4.6	32
6	4.6 ~ 5.4	32
7	5.4 ~ 6.3	32
8	6.3 ~ 7.3	32
9	7.3 ~ 8.5	32
10	8.5 ~ 10.0	32

$\Sigma=320$

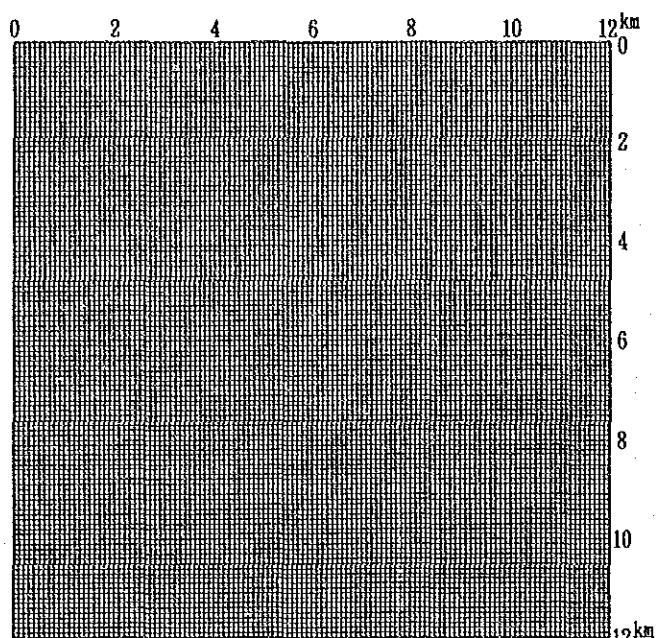
[FAR]

Data Grid Interval = 3,000 m

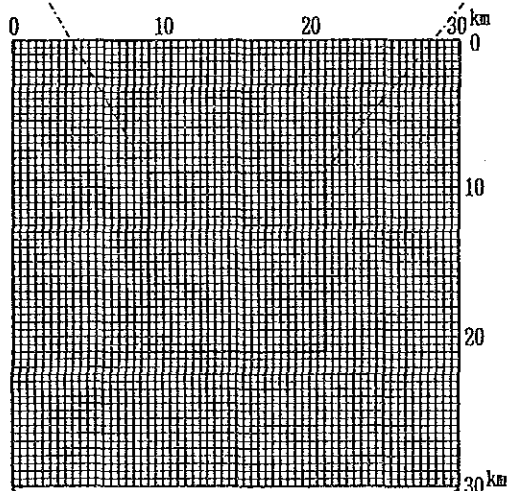
No.	Distance from Station	Number of Block
1	10.0 ~ 12.0 ^{km}	36
2	12.0 ~ 14.5	36
3	14.5 ~ 17.0	36
4	17.0 ~ 20.0	36
5	20.0 ~ 23.5	36
6	23.5 ~ 27.5	36
7	27.5 ~ 32.0	36
8	32.0 ~ 37.0	36
9	37.0 ~ 43.0	36
10	43.0 ~ 50.0	36

$\Sigma=360$

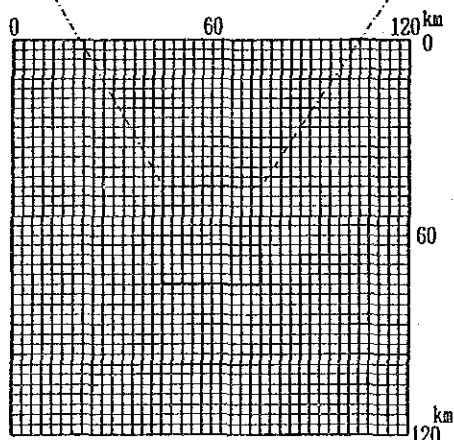
Fig II-3 Annular Segment for Terrain Correction



NEAR

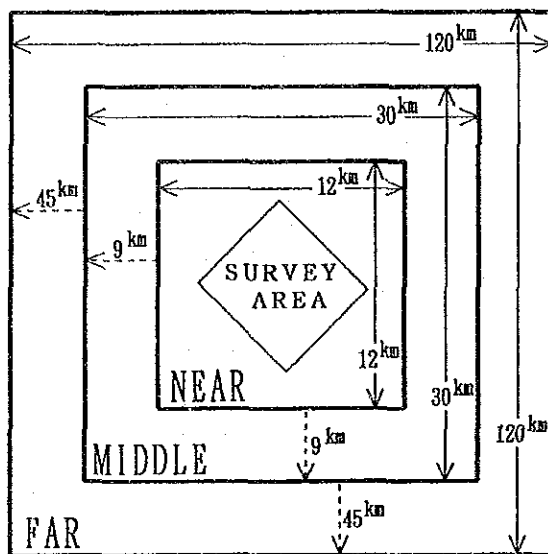


MIDDLE



FAR

DIVISION OF CORRECTION AREA

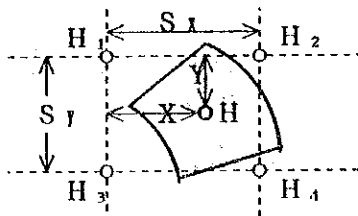


	NEAR	MIDDLE	FAR
Area	12×12 =144 km ²	30×30 =900 km ²	120×120 =14,400km ²
Grid interval	100 m	500 m	3,000 m
Number of grids	120×120 = 14,400	60×60 = 3,600	40×40 = 1,600
Scale of map	1:25,000	1:100,000	1:100,000

Fig II-4 Division of Terrain Correction Area

n : number of divided compartment
in a same circular ring.

The average altitude of each compartment H is estimated from the surrounding four altitude data values, H1, H2, H3, and H4, as follows:

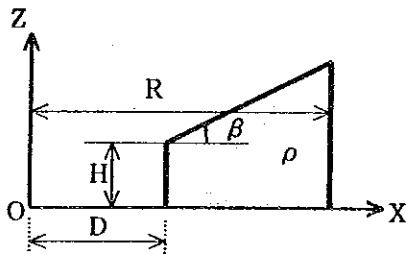


$$H = H_1 + (H_2 - H_1) X / S_1 + (H_3 - H_1) Y / S_2 + (H_1 + H_4 - H_2 - H_3) XY / S_1 S_2$$

(2) Sketch correction

We sketched the topographic features along the direction of maximum topographic undulation in a radius of 30m. Using the sketches, we calculated the sketch correction by Hiroshima's method. The expression and the schematic map are as follows:

$$\Delta g = 2 G \rho \int_D^R \left\{ \tanh^{-1} \sqrt{(R^2 - X^2) / (R^2 + h^2)} - \tanh^{-1} \sqrt{(R^2 - X^2) / (R^2 + X \tan \beta + H - h - D \tan \beta)^2} \right\} dx$$



where,
 Δg : sketch correction value (mgal)
 G: gravitational constant
 ρ : correction density (g/cm³)
 D: distance from station to cliff (m)
 H: height of cliff (m)
 β : angle of inclination of cliff (°)
 R: referred range for calculation (30m)
 h: height of gravimeter's weight (0.15m).

4) Elevation correction

This correction consists of three parts: (g1) the free-air correction, which accounts for the fact that each station is a different distance from the earth's center and the datum plane, (g2) the Bouguer correction, which removes the effect of a presumed infinite slab of material between the horizontal plane of each station and the datum, and (g3) the atmosphere correction, which removes the effect of the atmosphere.

Free-air correction: free-air correction is estimated by following expression:

$$\Delta g_1 = g_0 \left(1 - R^2 / (R+H)^2 \right) = (2 g_0 H R + g_0 H^2) / (R+H)^2$$

$$\approx 0.3086 H \text{ (mgal)}$$

where, g_0 : gravity at mean sea-level
 H : altitude of station (m)
 R : average radius of the earth.

Bouguer correction: Bouguer correction can be expressed as,

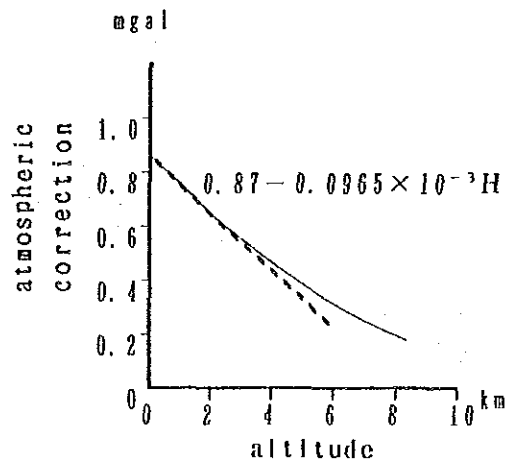
$$\Delta g_2 = -2 \pi G \rho H \approx -0.0419 \rho \cdot H \text{ (mgal)}$$

where, G : gravitational constant
 H : altitude of station (m)
 ρ : density of slab (g/cm³).

Atmosphere correction: an atmosphere correction can be obtained from the average atmospheric density model by use of the integral for the range 0 to 50 km. As shown in following figure, the relation between atmosphere correction and the altitude of the station can be assumed to be one-order function less than 3km of the altitude. Therefore, we can write as follows:

$$\Delta g_3 = 0.87 - 0.0965 \times 10^{-3} H \text{ (mgal)}$$

where, H : altitude of station (m).



Because free-air, Bouguer, and atmosphere corrections are functions of the altitude of the station, they are called elevation corrections and can be expressed as follows:

$$\text{Elevation correction: } \Delta g = \Delta g_1 + \Delta g_2 + \Delta g_3$$

$$= (0.3086 - 0.0419 \cdot \rho - 0.0965 \times 10^{-3}) H + 0.87$$

(mgal)

5) Latitude correction

Because of its rotation, the earth is not actually spherical. The shape can be approximated as an oblate spheroid with an eccentricity of 1/297. Both its departure from sphericity and its rotation cause the earth's gravitational acceleration to have a maximum value at the poles and a minimum at the equator. Therefore, the variation of gravity values with the latitude of the station is reduced by using following International Formula on the International Ellipsoid.

$$\gamma = (a \gamma_E \cos^2 \phi + b \gamma_P \sin^2 \phi) / (a^2 \cos^2 \phi + b^2 \sin^2 \phi)^{1/2} \text{ (mgal)}$$

where, a : equatorial radius of ellipsoid of revolution
 (6,378.14 km)
 b : equatorial radius of ellipsoid of revolution
 (6,356.18 km)
 γ_E : normal gravity value at the equator of ellipsoid of
 revolution(978.032 gal)
 γ_P : normal gravity value at the polar of ellipsoid of
 revolution(983.218 gal).

This is the International Gravity Formula of 1967, which is adopted by IUGG(International Union of Geodesy and Geophysics) as the expression giving the normal gravity.

Actually, we use the convenient following expression:

$$\gamma = 978, 031. 85 (1 + 0. 005278895 \sin^2 \phi + 0. 000023462 \sin^4 \phi) \text{ (mgal)}$$

6) Densities of rock samples

The terrain and Bouguer Corrections made in the reduction of gravity data require a knowledge of the densities of the rocks near the surface. To upgrade the precision of an analysis, an assumption of a detailed underground density structure is required.

In this survey, 35 rock samples were collected on the surface and from core samples and their wet densities were measured. The densities of rock samples can be obtained by using following expression:

$$\rho = \frac{Wa}{Wa - Ww}$$

where, ρ : density
 Wa: weight in air (after a day in water)
 Ww: weight in water

Table II-2 shows the results of measurement with main rocks.

7) Reduction density

Bulk densities for the thirty-five rock samples ranged from 2.43 to 2.70g/cm³. It is difficult to determine the formation density of these rocks from only their densities near the surface.

We determined a reduction density by the following methods in this survey.

i) Gravity contour maps were drawn for four densities, 2.2, 2.4, 2.67 and 2.80g/cm³. The correlation between gravity anomalies and topographic features are shown in following table. Fig.II-7 illustrates the gravity contour maps with densities of 2.67g/cm³, respectively.

	correlation between gravity anomaly and topographic feature			
	$\rho = 2.5$	$\rho = 2.6$	$\rho = 2.67$	$\rho = 2.8$
High gravity and High altitude or Low gravity and Low altitude	9	7	4	0
High gravity and Low altitude or Low gravity and High altitude	0	3	6	9

The density value at which the topographic features have the least observable effect on the gravity contours is considered to be most nearly correct. Therefore, correct density appears to be about 2.67g/cm³.

ii) The average density of the thirty-five rock samples is estimated to be 2.60g/cm³.

iii) Gravity is a function of altitude of station. When the altitudes and the corrected gravity values (after latitude and terrain corrections and reduction of gravity trends) are plotted on X-Y coordinates, the inclination of fitting lines represent the average of rock densities in the area. Fig.II-5 shows the relation of gravity versus altitude (G-H relation) for this sur-

GRAVIM. SURVEY OF PERU (G-H RELATION, ZERO ORDER TREND) SEP. 12, 1990
DENSITY = 2.673

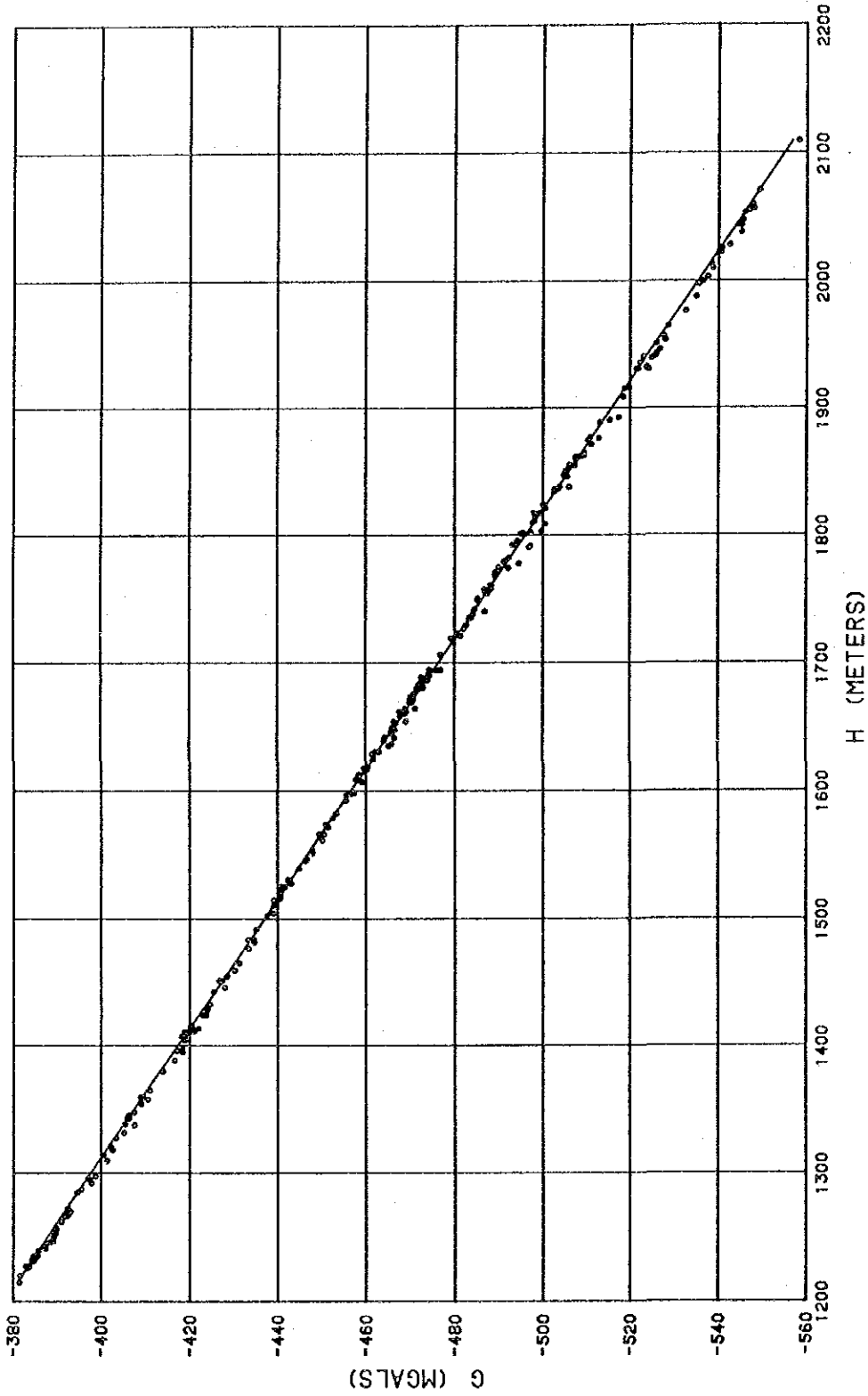


Fig II-5 Gravity versus Height Relation

vey and a density was estimated as 2.673g/cm³ by least squares method.

Eventually, a correction density of 2.4g/cm³ was arrived at from the density derived from the correlation between topographic features and gravity anomalies (2.67g/cm³), the average density of rocksamples (2.60g/cm³), and the density determined from the G-H relation (2.673g/cm³).

1-1-5 Interpretation

The extraction of anomalies associated with individual sub-surface sources from an observed gravitational field requires filtering operations. In this survey, we used the following techniques; surface fit analysis, and spectral analysis. Techniques developed by Talwani were also used to estimate two-dimensional density structures.

1) Surface fit analysis

Gravity contour maps frequently contain not only gravity anomalies produced by local geologic features but also gravity trends resulting from regional features.

In this area, gravity trends decrease from the northeast to the southwest. Therefore, a first-order approximate plane Z(X,Y) was adapted to remove the regional gravity trend.

Considering gravity data at grid points G(X,Y), we estimated a first-order surface fitting plane Z(X,Y) by the least squares method. Z(X,Y) and the residual values are presented in the following form:

$$Z (X, Y) = -141.85129 - 0.0403031 X + 0.0455303 Y$$

$$(\text{Residual Value}) = G (X, Y) - Z (X, Y)$$

The results are shown in Fig.II-8.

2) Spectral analysis

The gravity contour maps produced by this survey include anomalies of various wave lengths. By transforming such spatial gravity anomalies into the frequency domain, it is possible to estimate the average depth of the sources of anomalies and to eliminate gravity anomalies attracted by the source with spontaneous average depth (Spector and Grant, 1970).

Fig.II-6 shows the logarithmic energy spectrum of the gravity as a function of frequency, f(cycle/km), where the spectrum can be approximated by using two regression lines. From the gradients of these lines, the average depth (H) of buried sources can be expressed by following formula:

$$H = - \frac{1}{4\pi} \cdot \frac{\Delta \log E}{\Delta f}$$

In this survey, the gravity field can be separated into a regional component (Hr) with an average source depth of 1,240m, a near-surface component (HN=170m), and a middle component (KX=340m).

From the results of spectral analysis, we can draw spectral maps for the regional and near-surface components. In practice, the regional component, GR, is expressed mathematically by using two average depths, HR and HN, and KX, where difference of crossing points between energy spectral axis and each regression line.

$$G_R (X, Y) = \frac{\int_{-\infty}^{\infty} \int_{-\infty}^{\infty} G(\xi, \eta) \cdot W(X-\xi, Y-\eta) d\xi d\eta}{\int_{-\infty}^{\infty} \int_{-\infty}^{\infty} W(\xi, \eta) d\xi d\eta}$$

where, the weight function, W, can be expressed as follows:

$$W(X, Y) = \frac{1}{2\pi} \int_0^{\infty} \frac{f \cdot J_0(p \cdot f)}{1 + K_X \cdot e^{(H_R - H_N) \cdot f}} df$$

in which, $p^2 = X^2 + Y^2$

J₀: Bessel function.

The gravitational effect of shallow structures, GN(X,Y), is obtained through spectral analysis, by subtracting the regional component of the observed field, GR(X,Y), from the total observed gravitational field, G(X,Y) as follows:

$$G_N (X, Y) = G (X, Y) - G_R (X, Y)$$

3) Two-dimensional simulation

A two-dimensional simulation was carried out along two sections where two-dimensionality could be assumed in the subsurface structural configuration.

Two-dimensional bodies were represented by polygons and the gravitational attraction caused by these bodies was compared

LOGARITHMIC ENERGY SPECTRUMS

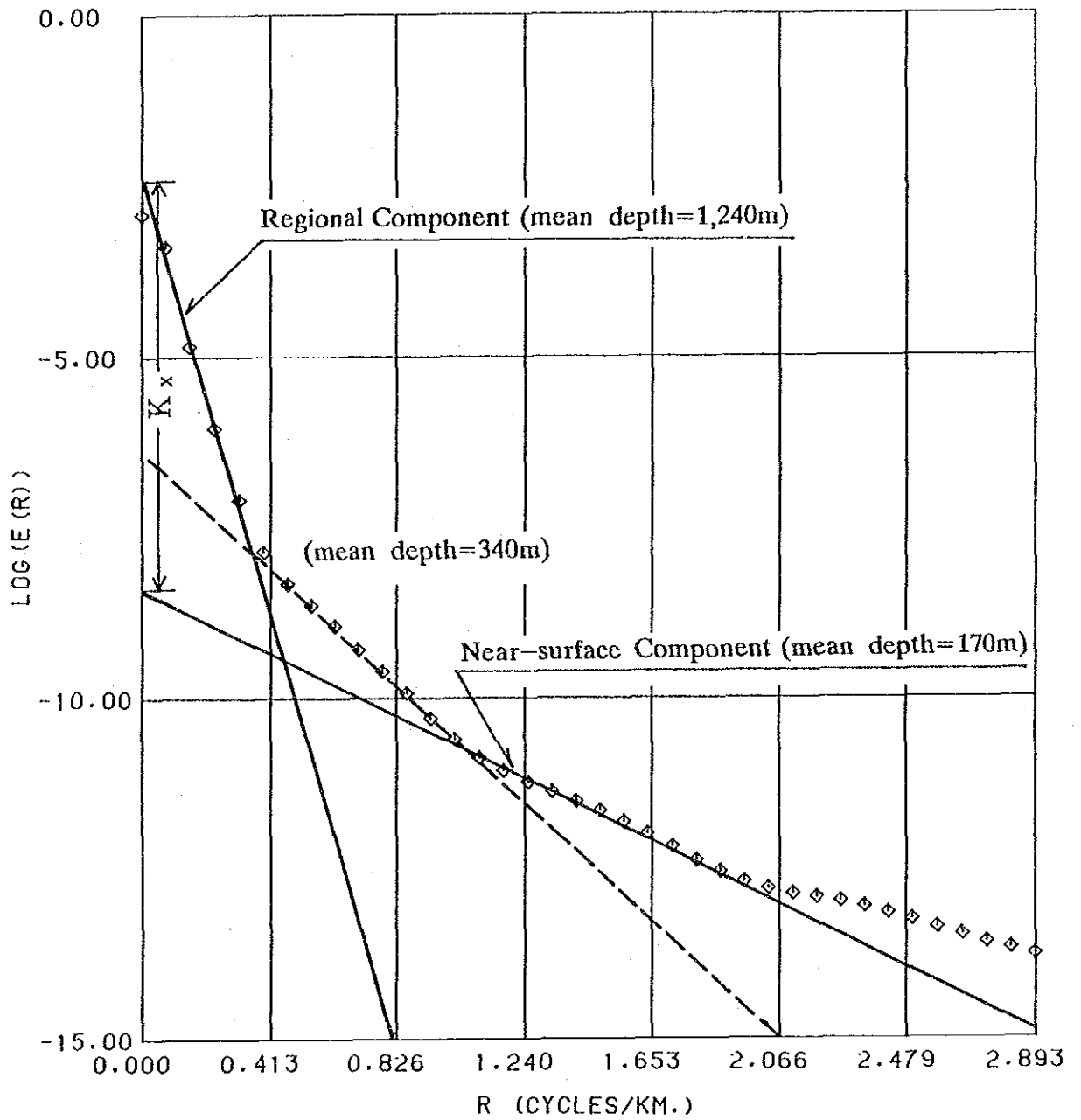


Fig II-6 Energy Spectrum

Table II-3 List of Gravity Data

(density for correction $\rho = 2.67 \text{ g/cm}^3$)

LEGEND

ST. NO	station number	
OBS. DAY	date of observation	
LAT.	latitude	
LONG.	longitude	
LEVEL	altitude of station (m)	
ABS. G	absolute gravity (gal)	
C. 30M	sketch correction (mgal)	
ETC	leveling method and gravimeter	L: leveling LG: L&R G-type
TERR. C	total terrain correction (mgal)	
F. E. C	Free-air correction (mgal)	
B. G. C	Bouguer correction (mgal)	
NORM. G	normal gravity (mgal)	
ANOM. F	Free-air anomaly (mgal)	
ANOM. B	Bouguer anomaly (mgal)	

ST.NO	OBS.DAY	LAT.	LONG.	LEVEL	ABS.G	C.20M	ETC	*	TERR.C	F.E.C	B.G.C	NORM.G	ANOM.F	ANOM.B
1	90 716	-543.35	-79 2.76	1215.04	977.687842	0.240	L	LG *	13.953	375.714	-134.279	978.083183	-5.674	-139.953
2	90 716	-543.33	-79 3.01	1227.31	977.685615	0.093	L	LG *	13.907	379.699	-135.618	978.083177	-4.156	-139.774
3	90 716	-543.17	-79 3.07	1236.62	977.684817	0.120	L	LG *	12.958	382.372	-136.634	978.083129	-2.983	-139.617
4	90 716	-543.13	-79 3.20	1227.55	977.685191	0.027	L	LG *	14.595	379.573	-135.644	978.083117	-3.753	-139.402
5	90 716	-542.95	-79 3.29	1232.79	977.683744	0.0	L	LG *	15.081	381.190	-136.216	978.083054	-3.049	-139.265
6	90 716	-542.83	-79 3.41	1226.30	977.683719	0.0	L	LG *	16.024	379.188	-135.508	978.083038	-4.097	-139.605
7	90 716	-542.71	-79 3.56	1242.10	977.680287	0.053	L	LG *	15.568	384.062	-137.232	978.082992	-3.074	-140.306
8	90 716	-542.62	-79 3.78	1255.13	977.676336	0.087	L	LG *	16.811	388.082	-138.653	978.082966	-1.736	-140.389
9	90 716	-542.50	-79 3.91	1246.36	977.677704	0.027	L	LG *	16.687	385.376	-137.696	978.082930	-3.164	-140.860
10	90 716	-542.38	-79 4.10	1252.83	977.676690	0.053	L	LG *	16.492	387.372	-138.402	978.082894	-2.340	-140.742
11	90 716	-542.24	-79 4.23	1252.68	977.677914	0.013	L	LG *	15.419	387.326	-138.386	978.082853	-2.194	-140.580
12	90 716	-542.18	-79 4.43	1247.24	977.677285	0.040	L	LG *	16.445	385.648	-137.792	978.082835	-3.457	-141.249
13	90 716	-542.07	-79 4.50	1253.33	977.677308	0.080	L	LG *	15.863	387.527	-138.457	978.082802	-2.104	-140.561
14	90 716	-541.93	-79 4.68	1251.86	977.675551	0.120	L	LG *	17.800	387.073	-138.296	978.082761	-2.336	-140.632
15	90 716	-541.73	-79 4.78	1269.96	977.673714	0.0	L	LG *	15.822	392.657	-140.270	978.082701	-0.508	-140.779
16	90 716	-541.61	-79 4.87	1267.73	977.673105	0.080	L	LG *	17.508	391.959	-140.027	978.082666	-0.083	-140.110
17	90 716	-541.45	-79 4.85	1269.71	977.674124	0.027	L	LG *	16.026	392.580	-140.243	978.082618	0.112	-140.131
18	90 716	-541.22	-79 4.89	1261.81	977.675618	0.0	L	LG *	15.893	390.143	-139.382	978.082550	-0.897	-140.278
19	90 716	-541.03	-79 4.95	1266.83	977.674055	0.0	L	LG *	16.044	391.691	-139.929	978.082494	-0.703	-140.632
20	90 717	-543.07	-79 2.37	1231.50	977.684591	0.0	L	LG *	13.871	380.792	-136.075	978.083100	-3.846	-139.921
21	90 718	-542.89	-79 2.46	1234.35	977.684301	0.013	L	LG *	13.909	381.671	-136.386	978.083046	-3.165	-139.551
22	90 718	-542.84	-79 2.64	1231.65	977.684616	0.107	L	LG *	14.085	380.838	-136.092	978.083031	-3.491	-139.583
23	90 718	-542.84	-79 2.83	1233.59	977.684501	0.093	L	LG *	13.492	381.492	-136.303	978.083031	-3.601	-139.904
24	90 718	-542.76	-79 2.91	1235.39	977.684195	0.080	L	LG *	14.164	381.992	-136.500	978.083007	-2.656	-139.155
25	90 718	-542.70	-79 3.00	1227.61	977.684397	0.227	L	LG *	15.776	379.592	-135.651	978.082990	-3.225	-138.876
26	90 718	-542.63	-79 3.11	1220.33	977.684788	0.133	L	LG *	16.602	377.346	-134.856	978.082969	-4.233	-139.089
27	90 718	-542.58	-79 3.23	1239.70	977.681661	0.120	L	LG *	15.539	383.322	-136.970	978.082954	-2.432	-139.402
28	90 718	-542.51	-79 3.35	1227.16	977.683376	0.0	L	LG *	16.330	379.453	-135.602	978.082933	-3.773	-139.375
29	90 718	-542.45	-79 3.47	1235.95	977.682046	0.013	L	LG *	15.289	382.165	-136.561	978.082915	-3.415	-139.976
30	90 718	-542.44	-79 3.58	1245.32	977.679894	0.013	L	LG *	15.407	385.056	-137.583	978.082912	-2.556	-140.139
31	90 718	-542.43	-79 3.73	1249.88	977.678926	0.053	L	LG *	14.637	386.462	-138.080	978.082909	-2.884	-140.964
32	90 718	-542.33	-79 3.86	1248.06	977.675675	0.040	L	LG *	14.462	392.071	-140.063	978.082879	-0.672	-140.735
33	90 718	-542.19	-79 3.92	1256.73	977.677755	0.040	L	LG *	15.275	388.576	-138.828	978.082838	-1.232	-140.060
34	90 718	-542.07	-79 4.02	1272.25	977.675379	0.040	L	LG *	14.924	393.364	-140.520	978.082802	0.864	-139.656
35	90 718	-541.96	-79 4.15	1287.22	977.672730	0.214	L	LG *	14.403	397.982	-142.152	978.082770	2.345	-139.807
36	90 718	-541.83	-79 4.25	1295.72	977.672628	0.160	L	LG *	12.937	400.604	-143.078	978.082731	3.438	-139.840
37	90 718	-541.73	-79 4.35	1319.81	977.668021	0.334	L	LG *	12.270	408.036	-145.703	978.082701	5.625	-140.078
38	90 718	-541.60	-79 4.39	1342.65	977.663858	0.107	L	LG *	12.451	415.082	-148.190	978.082663	8.728	-139.461
39	90 718	-541.42	-79 4.31	1338.18	977.664051	0.280	L	LG *	13.097	413.703	-147.703	978.082609	8.242	-139.461
40	90 718	-541.36	-79 4.47	1364.41	977.658798	0.320	L	LG *	12.684	421.795	-150.558	978.082592	10.686	-139.462
41	90 718	-541.18	-79 4.52	1409.75	977.650278	0.133	L	LG *	12.505	435.783	-154.490	978.082538	16.028	-139.462
42	90 718	-540.97	-79 4.56	1415.47	977.649614	0.053	L	LG *	12.382	437.547	-156.112	978.082476	17.067	-139.045
43	90 718	-540.84	-79 4.64	1411.35	977.649213	0.147	L	LG *	12.996	436.276	-155.664	978.082438	16.048	-139.616
44	90 718	-540.72	-79 4.71	1404.51	977.649722	0.067	L	LG *	12.936	434.166	-154.920	978.082402	15.221	-139.699
45	90 719	-542.85	-79 2.33	1241.63	977.681571	0.0	L	LG *	14.016	383.917	-137.180	978.083034	-3.529	-140.710
46	90 719	-542.77	-79 2.24	1292.14	977.673256	0.053	L	LG *	11.837	399.500	-142.688	978.083010	1.582	-141.106
47	90 719	-542.67	-79 2.19	1318.02	977.668796	0.013	L	LG *	11.473	407.484	-145.508	978.082981	4.772	-140.736
48	90 719	-542.55	-79 2.18	1357.37	977.661717	0.013	L	LG *	10.548	419.623	-149.792	978.082945	8.943	-140.849
49	90 719	-542.45	-79 2.20	1388.24	977.656297	0.0	L	LG *	9.965	429.147	-153.151	978.082915	12.494	-140.657
50	90 719	-542.35	-79 2.25	1428.02	977.649571	0.0	L	LG *	9.408	441.419	-157.476	978.082885	17.513	-139.963

ST.NO	OBS.DAY	LAT.	LONG.	LEVEL	ABS.G	C.20M	ETC	TERR.C	F.E.C	B.G.C	NORM.G	ANOM.F	ANOM.B
51	90 719	-542.25	-79 2.24	1465.18	977.642844	0.080	L	8.738	452.883	-161.513	978.082856	21.610	-139.903
52	90 719	-542.13	-79 2.32	1515.78	977.634351	0.067	L	7.948	468.493	-167.005	978.082820	27.971	-139.034
53	90 719	-542.03	-79 2.30	1551.57	977.627415	0.133	L	7.568	479.535	-170.886	978.082790	31.527	-139.359
54	90 719	-541.97	-79 2.36	1566.10	977.625082	0.0	L	7.049	484.017	-172.461	978.082773	33.376	-139.085
55	90 719	-541.88	-79 2.39	1592.38	977.620240	0.0	L	7.011	492.125	-175.308	978.082746	36.631	-138.678
56	90 719	-541.81	-79 2.44	1618.61	977.615331	0.027	L	7.036	500.217	-178.149	978.082725	39.858	-138.290
57	90 719	-541.74	-79 2.50	1646.61	977.609990	0.0	L	6.962	508.855	-181.179	978.082704	43.102	-138.076
58	90 719	-542.10	-79 2.41	1518.47	977.633435	0.227	L	8.756	469.325	-167.297	978.082811	28.702	-138.594
59	90 719	-542.20	-79 2.42	1529.22	977.631248	0.374	L	8.729	472.640	-168.463	978.082841	29.775	-138.687
60	90 719	-542.20	-79 2.50	1578.91	977.621355	0.414	L	8.906	487.969	-173.849	978.082841	35.389	-138.460
61	90 719	-542.24	-79 2.56	1608.39	977.615510	0.0	L	9.034	497.064	-177.042	978.082853	38.755	-138.287
62	90 719	-542.31	-79 2.54	1598.43	977.615638	0.147	L	9.862	493.991	-175.964	978.082874	36.617	-139.346
63	90 719	-542.39	-79 2.59	1582.58	977.618216	0.347	L	11.287	489.101	-174.247	978.082897	35.707	-138.540
64	90 719	-542.41	-79 2.67	1566.47	977.622135	0.254	L	11.181	484.131	-172.501	978.082903	34.544	-137.957
65	90 719	-542.48	-79 2.74	1530.81	977.628313	0.214	L	12.205	473.130	-168.635	978.082924	30.725	-137.911
66	90 719	-542.57	-79 2.73	1491.67	977.635225	0.414	L	12.619	461.055	-164.389	978.082951	25.949	-138.440
67	90 719	-542.68	-79 2.70	1428.91	977.646410	0.214	L	12.611	441.694	-157.573	978.082984	17.732	-139.841
68	90 719	-542.67	-79 2.62	1396.23	977.654017	0.214	L	11.783	431.612	-154.020	978.082981	14.431	-139.588
69	90 719	-542.64	-79 2.52	1347.49	977.663637	0.307	L	11.808	416.575	-148.717	978.082972	9.049	-139.668
70	90 719	-542.68	-79 2.45	1320.85	977.668453	0.214	L	12.362	408.357	-145.816	978.082984	6.168	-139.649
71	90 719	-542.71	-79 2.36	1294.94	977.673331	0.0	L	12.161	400.364	-142.993	978.082992	2.863	-140.150
72	90 719	-542.80	-79 2.40	1269.75	977.677554	0.027	L	12.592	392.592	-140.247	978.083019	-0.292	-140.539
73	90 720	-541.64	-79 2.52	1661.44	977.609338	0.040	L	6.760	513.430	-182.783	978.082675	44.453	-138.350
74	90 720	-541.57	-79 2.54	1694.20	977.600208	0.040	L	6.537	523.537	-186.325	978.082654	47.629	-138.656
75	90 720	-541.50	-79 2.53	1721.27	977.594869	0.013	L	6.468	531.888	-189.250	978.082633	50.611	-138.659
76	90 720	-541.41	-79 2.59	1729.83	977.593574	0.0	L	6.400	534.529	-190.175	978.082606	51.897	-138.278
77	90 720	-541.26	-79 2.57	1735.61	977.592296	0.133	L	6.537	536.312	-190.799	978.082562	52.583	-138.216
78	90 720	-541.18	-79 2.53	1760.32	977.587383	0.0	L	6.795	543.935	-193.467	978.082538	55.555	-137.912
79	90 720	-541.06	-79 2.47	1750.33	977.589495	0.027	L	7.819	540.853	-192.388	978.082503	55.664	-136.775
80	90 720	-541.04	-79 2.38	1770.75	977.585705	0.027	L	7.591	547.153	-194.592	978.082497	57.952	-136.640
81	90 720	-540.93	-79 2.32	1814.57	977.575687	0.080	L	8.553	560.671	-199.319	978.082464	62.447	-136.872
82	90 720	-541.09	-79 2.21	1768.23	977.586155	0.214	L	7.210	546.375	-194.320	978.082512	57.228	-137.092
83	90 720	-541.09	-79 2.05	1719.64	977.596089	0.040	L	7.232	531.385	-189.074	978.082512	52.194	-136.880
84	90 720	-541.13	-79 1.91	1688.71	977.602017	0.040	L	7.922	521.843	-185.732	978.082524	49.259	-136.473
85	90 720	-541.29	-79 1.91	1694.56	977.601317	0.013	L	6.874	523.648	-186.364	978.082571	49.268	-137.096
86	90 720	-541.36	-79 2.08	1682.98	977.603824	0.040	L	6.827	520.075	-185.112	978.082592	48.135	-136.978
87	90 720	-541.49	-79 2.14	1668.94	977.605980	0.027	L	6.628	515.744	-183.594	978.082630	45.772	-137.822
88	90 720	-541.57	-79 2.24	1652.84	977.608944	0.107	L	6.906	510.777	-181.853	978.082654	43.973	-137.879
89	90 720	-541.60	-79 2.36	1630.81	977.613144	0.254	L	7.246	503.981	-179.469	978.082663	41.707	-137.762
90	90 720	-541.68	-79 2.42	1640.01	977.611544	0.0	L	6.870	506.819	-180.465	978.082687	42.546	-137.919
91	90 721	-541.78	-79 2.56	1616.98	977.614884	0.187	L	7.647	499.714	-177.972	978.082716	39.529	-138.443
92	90 721	-541.83	-79 2.62	1616.16	977.614907	0.0	L	7.941	499.461	-177.883	978.082731	39.578	-138.305
93	90 721	-541.90	-79 2.61	1624.77	977.612510	0.414	L	8.477	503.117	-178.815	978.082752	40.352	-138.463
94	90 721	-541.99	-79 2.59	1630.84	977.611108	0.080	L	8.615	503.990	-179.472	978.082779	40.934	-138.538
95	90 721	-542.07	-79 2.59	1647.80	977.606679	0.374	L	9.472	509.222	-181.308	978.082802	42.570	-138.737
96	90 721	-542.16	-79 2.60	1660.55	977.603636	0.040	L	10.221	513.155	-182.687	978.082829	44.184	-138.502
97	90 721	-542.24	-79 2.64	1664.20	977.603039	0.200	L	10.912	514.282	-183.082	978.082853	45.379	-137.702
98	90 721	-542.22	-79 2.71	1662.51	977.602839	0.214	L	11.899	513.760	-182.899	978.082847	44.651	-138.248
99	90 721	-542.22	-79 2.79	1669.19	977.600451	0.414	L	11.973	515.821	-183.621	978.082847	45.398	-138.223
100	90 721	-542.18	-79 2.84	1671.24	977.600146	0.294	L	11.895	516.453	-183.843	978.082835	45.660	-138.183

ST.NO	OBS.DAY	LAT.	LONG.	LEVEL	ABS.G	C.20M	ETC	TERR.C	F.E.C	B.G.C	NORM.G	ANOM.F	ANOM.B
101	90 721	-542.17	-79 2.89	1658.41	977.602976	0.294	L	12.046	512.495	-182.455	978.082832	44.685	-137.770
102	90 721	-542.19	-79 2.95	1647.61	977.604166	0.400	L	12.670	509.163	-181.287	978.082838	43.161	-138.126
103	90 721	-542.20	-79 3.02	1645.57	977.603604	0.133	L	13.346	508.534	-181.066	978.082841	42.644	-138.422
104	90 721	-542.15	-79 3.00	1639.29	977.606856	0.374	L	12.006	506.597	-180.387	978.082826	42.433	-137.954
105	90 721	-542.07	-79 3.04	1642.07	977.606219	0.441	L	12.191	507.454	-180.888	978.082802	43.062	-137.625
106	90 721	-542.01	-79 3.07	1654.28	977.604214	0.267	L	12.162	511.221	-182.009	978.082784	44.812	-137.196
107	90 721	-541.96	-79 3.13	1671.04	977.600861	0.200	L	11.928	516.392	-183.821	978.082770	46.411	-137.410
108	90 721	-541.92	-79 3.18	1676.00	977.600135	0.254	L	11.715	517.922	-184.358	978.082758	47.014	-137.344
109	90 721	-541.89	-79 3.24	1685.75	977.598426	0.280	L	11.532	520.930	-185.412	978.082749	48.139	-137.273
110	90 721	-541.87	-79 3.31	1686.60	977.598713	0.174	L	11.281	521.192	-185.504	978.082743	48.443	-137.060
111	90 721	-541.82	-79 3.36	1683.32	977.599596	0.200	L	10.866	520.180	-185.149	978.082728	47.915	-137.234
112	90 721	-541.75	-79 3.36	1680.26	977.601064	0.200	L	10.072	519.236	-184.818	978.082707	47.664	-137.154
113	90 721	-541.70	-79 3.40	1673.75	977.603164	0.107	L	9.389	517.228	-184.114	978.082692	47.088	-137.026
114	90 721	-541.67	-79 3.46	1681.76	977.601356	0.053	L	9.132	519.699	-184.980	978.082684	47.503	-137.477
115	90 721	-541.64	-79 3.53	1686.76	977.599898	0.0	L	8.777	521.241	-185.521	978.082675	47.242	-138.279
116	90 721	-541.57	-79 3.59	1680.67	977.601142	0.0	L	8.578	519.563	-184.862	978.082654	46.429	-138.433
117	90 721	-541.49	-79 3.61	1681.76	977.601234	0.027	L	8.520	519.699	-184.980	978.082650	46.822	-138.158
118	90 721	-541.40	-79 3.60	1689.94	977.599437	0.133	L	8.841	522.222	-185.865	978.082604	47.897	-137.968
119	90 721	-541.32	-79 3.59	1689.24	977.599291	0.107	L	9.421	522.006	-185.789	978.082580	48.139	-137.650
120	90 721	-541.25	-79 3.64	1688.20	977.599287	0.093	L	9.320	521.686	-185.677	978.082559	47.733	-137.943
121	90 721	-541.18	-79 3.60	1706.59	977.595502	0.027	L	10.428	527.359	-187.664	978.082538	50.551	-137.113
122	90 721	-541.21	-79 3.72	1661.80	977.605014	0.187	L	9.912	513.454	-182.822	978.082547	45.920	-136.902
123	90 721	-541.20	-79 3.82	1629.09	977.609801	0.347	L	11.194	503.450	-179.283	978.082544	41.901	-137.382
124	90 721	-541.16	-79 3.89	1612.71	977.612444	0.174	L	11.651	498.597	-177.510	978.082532	39.959	-137.551
125	90 721	-541.14	-79 3.97	1608.97	977.613309	0.027	L	11.465	497.243	-177.105	978.082526	39.490	-137.615
126	90 721	-541.12	-79 4.05	1610.58	977.612815	0.280	L	11.545	497.740	-177.279	978.082521	39.579	-137.700
127	90 721	-541.13	-79 4.13	1596.89	977.615552	0.133	L	11.255	493.516	-175.797	978.082524	37.799	-137.997
128	90 721	-541.17	-79 4.21	1574.18	977.620388	0.347	L	11.064	486.510	-173.337	978.082535	35.427	-137.910
129	90 721	-541.18	-79 4.32	1571.71	977.619649	0.013	L	11.340	485.767	-173.076	978.082538	34.217	-138.858
130	90 721	-541.16	-79 4.40	1527.95	977.628218	0.133	L	11.143	472.248	-168.325	978.082532	29.076	-139.249
131	90 723	-541.31	-79 2.67	1757.65	977.587829	0.013	L	6.522	543.111	-193.179	978.082577	54.885	-138.293
132	90 723	-541.23	-79 2.72	1760.78	977.587418	0.0	L	7.087	544.077	-193.516	978.082553	56.028	-137.488
133	90 723	-541.15	-79 2.81	1779.73	977.583580	0.027	L	7.475	549.923	-195.561	978.082529	58.448	-137.113
134	90 723	-541.19	-79 2.87	1810.90	977.577014	0.013	L	7.488	559.539	-198.923	978.082541	61.500	-137.423
135	90 723	-541.14	-79 2.91	1836.41	977.571993	0.0	L	7.898	567.499	-201.673	978.082526	64.774	-136.900
136	90 723	-541.09	-79 2.95	1852.52	977.568774	0.013	L	7.985	572.379	-203.409	978.082512	66.626	-136.783
137	90 723	-541.03	-79 2.99	1877.02	977.563656	0.0	L	7.984	579.937	-206.048	978.082494	69.084	-136.964
138	90 723	-541.01	-79 3.06	1915.29	977.555300	0.187	L	8.510	591.744	-210.167	978.082488	73.066	-137.101
139	90 723	-540.96	-79 3.11	1950.86	977.548091	0.013	L	8.395	602.717	-213.992	978.082473	76.729	-137.263
140	90 723	-540.92	-79 3.19	2003.22	977.535827	0.147	L	9.090	618.870	-219.619	978.082461	81.326	-138.293
141	90 723	-540.86	-79 3.24	2038.09	977.527117	0.040	L	10.115	629.688	-223.362	978.082444	84.416	-138.946
142	90 723	-540.81	-79 3.28	2028.35	977.529431	0.174	L	10.452	626.623	-222.317	978.082429	84.076	-138.240
143	90 723	-540.77	-79 3.35	2009.89	977.532469	0.454	L	11.124	620.928	-220.335	978.082417	82.104	-138.231
144	90 723	-540.76	-79 3.43	1999.80	977.534306	0.120	L	11.684	617.815	-219.251	978.082414	81.391	-137.861
145	90 723	-540.76	-79 3.49	1987.85	977.537042	0.150	L	10.438	614.159	-217.968	978.082414	79.195	-138.773
146	90 723	-540.73	-79 3.55	1976.49	977.539508	0.133	L	10.335	610.624	-216.747	978.082405	78.062	-138.685
147	90 723	-540.76	-79 3.60	1943.18	977.547006	0.067	L	9.439	600.348	-213.167	978.082414	74.379	-138.788
148	90 723	-540.81	-79 3.54	1916.16	977.552941	0.307	L	9.671	592.018	-210.263	978.082429	72.201	-138.061
149	90 723	-540.86	-79 3.48	1890.63	977.557568	0.374	L	9.622	584.136	-207.513	978.082444	68.883	-138.650
150	90 723	-540.91	-79 3.44	1862.61	977.564145	0.027	L	9.316	575.492	-204.496	978.082458	66.494	-138.002

DENSITY = 2.67 (G/CM**3)

***** THE LIST OF GRAVITY SURVEY (PERU90) *****

90(YEAR)

ST.NO	OBS.DAY	LAT.	LONG.	LEVEL	ABS.G	C-20M	ETC	*	TERR.C	F.E.C	B.G.C	NORM.G	ANOM.F	ANOM.B
151	90 723	-540.98	-79 3.42	1864.80	977.564023	0.093	L	LG *	9.114	576.167	-204.732	978.082479	66.826	-137.906
152	90 723	-541.06	-79 3.41	1845.86	977.567628	0.254	L	LG *	9.389	570.324	-202.691	978.082503	64.839	-137.853
153	90 723	-541.14	-79 3.40	1838.11	977.569183	0.080	L	LG *	9.600	567.933	-201.856	978.082526	64.190	-137.867
154	90 723	-541.21	-79 3.43	1817.50	977.573571	0.067	L	LG *	9.673	561.575	-199.635	978.082547	62.272	-137.362
155	90 723	-541.28	-79 3.46	1817.35	977.573225	0.147	L	LG *	10.006	561.529	-199.619	978.082568	62.192	-137.427
156	90 723	-541.34	-79 3.51	1782.26	977.580683	0.067	L	LG *	9.615	550.703	-195.834	978.082586	58.416	-137.418
157	90 723	-541.43	-79 3.49	1741.76	977.589070	0.147	L	LG *	9.098	538.209	-191.463	978.082612	53.765	-137.698
158	90 723	-541.48	-79 3.51	1723.23	977.593107	0.093	L	LG *	8.781	532.492	-189.462	978.082627	51.753	-137.709
159	90 723	-541.56	-79 3.49	1716.76	977.594155	0.013	L	LG *	8.729	530.496	-188.763	978.082651	50.730	-138.033
160	90 723	-541.54	-79 3.43	1735.35	977.590491	0.013	L	LG *	8.898	536.232	-190.771	978.082645	52.975	-137.796
161	90 723	-541.56	-79 3.36	1748.92	977.588215	0.053	L	LG *	9.238	540.418	-192.236	978.082651	55.220	-137.016
162	90 723	-541.59	-79 3.30	1757.55	977.586430	0.160	L	LG *	9.550	543.080	-193.168	978.082660	56.400	-136.768
163	90 723	-541.63	-79 3.25	1774.85	977.582840	0.107	L	LG *	9.849	548.417	-195.035	978.082672	58.435	-136.600
164	90 723	-541.66	-79 3.20	1795.30	977.578205	0.133	L	LG *	10.285	554.726	-197.241	978.082681	60.536	-136.705
165	90 723	-541.71	-79 3.18	1822.75	977.571092	0.133	L	LG *	11.303	563.195	-200.201	978.082695	62.894	-137.306
166	90 723	-541.75	-79 3.14	1850.29	977.563956	0.160	L	LG *	13.677	571.691	-203.169	978.082707	66.616	-136.553
167	90 723	-541.79	-79 3.10	1855.50	977.562628	0.521	L	LG *	14.090	573.298	-203.730	978.082719	67.297	-136.433
168	90 723	-541.79	-79 3.05	1859.60	977.562592	0.334	L	LG *	12.651	574.563	-204.172	978.082722	67.088	-137.084
169	90 723	-541.80	-79 3.00	1862.19	977.561813	0.200	L	LG *	12.497	575.362	-204.451	978.082722	66.950	-137.501
170	90 723	-541.82	-79 2.94	1861.60	977.562421	0.053	L	LG *	12.920	575.180	-204.387	978.082728	67.793	-136.594
171	90 723	-541.78	-79 2.93	1855.13	977.563725	0.107	L	LG *	11.819	573.184	-203.690	978.082716	66.012	-137.678
172	90 723	-541.71	-79 2.93	1847.34	977.566000	0.374	L	LG *	11.986	570.781	-202.851	978.082695	66.072	-136.779
173	90 723	-541.65	-79 2.91	1834.45	977.569362	0.374	L	LG *	10.757	566.804	-201.462	978.082678	64.246	-137.216
174	90 723	-541.58	-79 2.93	1824.04	977.572436	0.334	L	LG *	10.161	563.593	-200.360	978.082657	63.533	-136.807
175	90 723	-541.53	-79 2.92	1801.74	977.577619	0.107	L	LG *	9.506	556.713	-197.936	978.082642	61.196	-136.739
176	90 723	-541.48	-79 2.90	1779.26	977.582586	0.013	L	LG *	8.820	549.778	-195.511	978.082627	58.556	-136.954
177	90 723	-541.42	-79 2.86	1755.80	977.587805	0.0	L	LG *	7.951	542.540	-192.979	978.082609	55.687	-137.292
178	90 723	-541.42	-79 2.78	1734.98	977.592293	0.0	L	LG *	7.032	536.117	-190.731	978.082609	52.834	-137.897
179	90 723	-541.41	-79 2.71	1729.97	977.593434	0.040	L	LG *	6.655	534.372	-190.190	978.082606	52.054	-138.136
180	90 723	-541.38	-79 2.62	1738.04	977.592058	0.0	L	LG *	6.433	537.061	-191.061	978.082598	52.965	-138.096
181	90 724	-542.75	-79 2.80	1285.14	977.674761	0.160	L	LG *	13.637	397.340	-141.925	978.083004	2.734	-139.191
182	90 724	-542.66	-79 2.82	1313.71	977.669916	0.027	L	LG *	12.399	406.154	-145.038	978.082978	5.492	-139.547
183	90 724	-542.62	-79 2.88	1327.37	977.667174	0.013	L	LG *	12.337	410.368	-146.526	978.082966	6.914	-139.612
184	90 724	-542.58	-79 2.96	1343.06	977.664254	0.200	L	LG *	12.767	415.209	-148.235	978.082954	9.276	-138.959
185	90 724	-542.54	-79 3.03	1345.18	977.663439	0.160	L	LG *	13.211	415.893	-148.465	978.082942	9.571	-138.895
186	90 724	-542.48	-79 3.13	1359.46	977.659718	0.254	L	LG *	14.221	420.268	-150.020	978.082924	11.283	-138.737
187	90 724	-542.41	-79 3.21	1416.21	977.648917	0.093	L	LG *	13.726	437.776	-156.192	978.082903	17.516	-138.676
188	90 724	-542.31	-79 3.25	1407.12	977.650850	0.147	L	LG *	13.143	434.971	-155.204	978.082874	16.091	-139.113
189	90 724	-542.24	-79 3.20	1451.21	977.642770	0.200	L	LG *	12.763	448.573	-159.996	978.082853	21.254	-138.742
190	90 724	-542.18	-79 3.19	1451.39	977.643072	0.053	L	LG *	13.063	448.629	-160.015	978.082835	21.930	-138.085
191	90 724	-542.22	-79 3.28	1407.54	977.650732	0.307	L	LG *	13.839	435.101	-155.250	978.082847	16.825	-138.425
192	90 724	-542.21	-79 3.35	1410.48	977.650031	0.237	L	LG *	13.806	436.008	-155.569	978.082844	17.001	-138.568
193	90 724	-542.20	-79 3.42	1413.03	977.649473	0.254	L	LG *	13.176	436.795	-155.847	978.082841	16.603	-139.243
194	90 724	-542.12	-79 3.40	1502.69	977.632267	0.280	L	LG *	12.883	464.455	-165.585	978.082817	26.788	-138.797
195	90 724	-542.04	-79 3.43	1520.42	977.629329	0.374	L	LG *	12.705	469.925	-167.508	978.082793	29.166	-138.542
196	90 724	-541.97	-79 3.48	1525.46	977.629125	0.374	L	LG *	12.673	471.480	-168.055	978.082773	30.505	-137.350
197	90 724	-541.94	-79 3.57	1524.86	977.628924	0.200	L	LG *	12.172	471.295	-167.990	978.082764	29.627	-138.363
198	90 724	-541.87	-79 3.63	1514.75	977.631389	0.227	L	LG *	12.158	468.176	-166.893	978.082743	28.980	-137.913
199	90 724	-541.88	-79 3.74	1539.41	977.626544	0.107	L	LG *	11.268	475.783	-169.568	978.082746	30.849	-138.718
200	90 724	-541.79	-79 3.71	1597.82	977.614984	0.080	L	LG *	10.935	493.803	-175.898	978.082719	37.003	-138.895

ST.NO	OBS.DAY	LAT.	LONG.	LEVEL	ABS.G	C.20M	ETC	TERR.C	F.E.C	B.G.C	NORM.G	ANOM.F	ANOM.B
201	90 724	-541.73	-79 3.67	1648.93	977.606194	0.013	L	10.520	509.571	-181.430	978.082701	43.584	-137.846
202	90 724	-541.70	-79 3.59	1680.39	977.600526	0.013	L	9.754	519.276	-184.832	978.082692	46.863	-137.969
203	90 724	-541.57	-79 3.66	1661.89	977.604698	0.027	L	8.646	513.569	-182.832	978.082654	44.259	-138.573
204	90 724	-541.54	-79 3.76	1645.15	977.607358	0.147	L	9.616	508.405	-181.021	978.082645	42.733	-138.288
205	90 724	-541.51	-79 3.85	1617.72	977.613615	0.093	L	9.443	499.942	-178.052	978.082636	40.364	-137.689
206	90 724	-541.71	-79 3.79	1582.36	977.619268	0.040	L	10.094	489.034	-174.223	978.082695	35.700	-138.523
207	90 724	-541.73	-79 3.88	1510.60	977.632738	0.107	L	10.856	466.895	-166.443	978.082701	27.788	-138.635
208	90 724	-541.77	-79 3.97	1454.42	977.643107	0.107	L	11.281	449.564	-160.344	978.082713	21.238	-139.106
209	90 724	-541.85	-79 4.05	1424.22	977.647983	0.174	L	11.774	440.247	-157.063	978.082737	17.267	-139.796
210	90 724	-541.95	-79 4.00	1358.97	977.650363	0.174	L	12.836	420.117	-149.966	978.082767	10.550	-139.417
211	90 725	-541.74	-79 2.65	1650.57	977.608841	0.027	L	7.610	510.077	-181.607	978.082704	43.824	-137.783
212	90 725	-541.79	-79 2.70	1660.81	977.608013	0.320	L	8.335	513.236	-182.715	978.082719	44.965	-137.750
213	90 725	-541.87	-79 2.74	1691.68	977.599303	0.374	L	9.227	522.759	-186.053	978.082743	48.546	-137.507
214	90 725	-541.95	-79 2.72	1726.75	977.590991	0.280	L	9.670	533.578	-189.842	978.082767	51.473	-138.369
215	90 725	-542.01	-79 2.70	1754.01	977.584439	0.174	L	11.013	541.988	-192.786	978.082784	54.656	-138.130
216	90 725	-542.11	-79 2.71	1774.19	977.577410	0.200	L	13.164	548.214	-194.964	978.082802	55.986	-138.977
217	90 725	-542.11	-79 2.70	1756.37	977.589737	0.147	L	14.523	542.716	-193.040	978.082814	55.163	-137.877
218	90 725	-542.08	-79 2.74	1800.91	977.571421	0.053	L	15.391	536.457	-197.846	978.082805	60.464	-137.382
219	90 725	-542.06	-79 2.78	1809.83	977.569845	0.107	L	15.325	539.209	-198.808	978.082799	61.580	-137.228
220	90 725	-542.03	-79 2.82	1802.12	977.573311	0.227	L	12.226	556.830	-197.977	978.082790	59.578	-138.399
221	90 725	-542.04	-79 2.90	1820.90	977.567383	0.307	L	14.779	562.624	-200.301	978.082793	61.593	-138.008
222	90 725	-541.97	-79 2.89	1836.54	977.565530	0.200	L	13.728	567.449	-201.687	978.082773	63.935	-137.752
223	90 725	-541.92	-79 2.90	1862.69	977.559098	0.120	L	14.231	575.516	-204.505	978.082758	66.107	-138.398
224	90 725	-541.87	-79 2.92	1871.41	977.557818	0.294	L	13.924	578.204	-205.444	978.082743	67.205	-138.238
225	90 725	-542.38	-79 2.34	1432.73	977.648654	0.280	L	9.907	442.872	-157.988	978.082894	18.340	-139.648
226	90 725	-542.45	-79 2.30	1422.65	977.651797	0.040	L	10.235	436.677	-155.805	978.082915	15.794	-140.011
227	90 725	-541.98	-79 3.62	1442.93	977.644420	0.093	L	12.890	446.019	-159.096	978.082776	20.553	-138.543
228	90 725	-542.06	-79 3.56	1411.08	977.650241	0.040	L	13.686	436.193	-155.635	978.082799	17.320	-138.314
229	90 725	-542.13	-79 3.66	1379.74	977.656325	0.067	L	12.442	426.525	-152.226	978.082820	12.471	-139.755
230	90 725	-542.18	-79 3.66	1354.04	977.661105	0.013	L	12.604	418.596	-149.430	978.082835	9.470	-139.960
231	90 725	-542.26	-79 3.68	1331.64	977.665134	0.0	L	12.508	411.686	-146.991	978.082859	6.470	-140.522
232	90 731	-541.92	-79 2.22	1553.82	977.627647	0.013	L	7.156	480.229	-171.130	978.082758	32.274	-138.856
233	90 731	-541.87	-79 2.08	1545.50	977.629931	0.027	L	7.386	477.662	-170.228	978.082743	31.336	-138.892
234	90 731	-541.90	-79 1.95	1546.47	977.628382	0.0	L	7.681	477.961	-170.333	978.082752	31.273	-139.061
235	90 731	-542.03	-79 1.84	1504.17	977.635623	0.013	L	8.136	464.912	-165.745	978.082790	25.880	-139.866
236	90 731	-542.00	-79 1.71	1476.55	977.640457	0.0	L	8.978	456.391	-162.748	978.082781	23.044	-139.703
237	90 731	-541.94	-79 1.61	1483.41	977.638795	0.0	L	9.419	458.307	-163.492	978.082764	23.958	-139.535
238	90 731	-541.93	-79 1.51	1459.60	977.642408	0.0	L	10.126	451.162	-160.907	978.082761	20.935	-139.972
239	90 731	-542.31	-79 1.71	1424.13	977.648825	0.013	L	10.401	440.219	-157.053	978.082874	16.572	-140.481
240	90 731	-542.20	-79 1.66	1446.19	977.644881	0.013	L	10.020	447.025	-159.450	978.082841	19.085	-140.365
241	90 731	-542.13	-79 1.83	1481.87	977.639435	0.0	L	8.711	458.032	-163.325	978.082820	23.358	-139.967
242	90 731	-542.29	-79 1.87	1413.53	977.651578	0.0	L	9.254	436.949	-155.901	978.082868	14.914	-140.987
243	90 731	-542.44	-79 1.87	1397.09	977.654367	0.0	L	10.152	431.877	-154.113	978.082912	13.483	-140.630
244	90 731	-542.38	-79 2.00	1395.15	977.654682	0.027	L	9.585	431.279	-153.902	978.082894	12.798	-141.104
245	90 731	-542.33	-79 2.12	1411.24	977.652595	0.013	L	9.379	436.242	-155.652	978.082879	15.337	-140.315
246	90 731	-541.06	-79 2.80	1792.04	977.581157	0.093	L	8.232	553.721	-196.889	978.082503	60.606	-136.283
247	90 731	-540.98	-79 2.73	1801.29	977.579242	0.040	L	8.262	556.574	-197.887	978.082479	61.599	-136.288
248	90 731	-540.87	-79 2.71	1817.54	977.575024	0.0	L	9.567	561.587	-199.639	978.082547	63.763	-135.877
249	90 731	-541.23	-79 2.94	1816.28	977.575552	0.013	L	8.662	561.199	-199.503	978.082553	62.860	-136.643
250	90 731	-541.26	-79 2.99	1874.93	977.562782	0.040	L	9.530	579.292	-205.823	978.082562	69.042	-136.780

DENSITY = 2.67 (G/CM**3)

***** THE LIST OF GRAVITY SURVEY (PERU90) *****

90(YEAR)

ST.NO	OBS.DAY	LAT.	LONG.	LEVEL	ABS.G	C.20M	ETC	TERR.C	F.E.C	B.G.C	NORM.G	ANDM.F	ANDM.B
251	90 8 1	-541.74	-79 3.08	1888.67	977.535036	0.320	L	14.650	583.531	-207.302	978.082704	70.513	-136.789
252	90 8 1	-541.68	-79 3.06	1935.83	977.544390	0.160	L	16.061	598.080	-212.376	978.082687	75.845	-136.531
253	90 8 1	-541.63	-79 3.07	1940.25	977.545076	0.133	L	14.557	599.444	-212.852	978.082672	76.405	-136.447
254	90 8 1	-541.59	-79 3.11	1931.00	977.548700	0.320	L	12.581	596.590	-211.857	978.082660	75.211	-136.646
255	90 8 1	-541.55	-79 3.11	1931.22	977.548521	0.374	L	12.315	596.658	-211.881	978.082648	74.847	-137.034
256	90 8 1	-541.53	-79 3.08	1964.67	977.540247	0.227	L	13.743	606.978	-215.477	978.082642	78.326	-137.151
257	90 8 1	-541.48	-79 3.08	1997.62	977.531612	0.254	L	15.477	617.143	-219.017	978.082627	81.605	-137.412
258	90 8 1	-541.42	-79 3.09	2013.19	977.527874	0.307	L	16.311	621.946	-220.689	978.082609	83.522	-137.167
259	90 8 1	-541.38	-79 3.11	2023.06	977.526355	0.254	L	16.083	624.991	-221.749	978.082598	84.831	-136.918
260	90 8 1	-541.33	-79 3.13	2025.72	977.526888	0.160	L	14.961	625.812	-222.035	978.082583	85.078	-136.956
261	90 8 1	-541.26	-79 3.14	2043.90	977.523557	0.214	L	15.519	631.420	-223.986	978.082562	86.934	-137.052
262	90 8 1	-541.21	-79 3.17	2055.42	977.519646	0.187	L	15.910	634.974	-225.222	978.082547	87.983	-137.238
263	90 8 1	-541.16	-79 3.20	2059.61	977.519057	0.227	L	15.635	636.267	-225.671	978.082532	88.426	-137.245
264	90 8 1	-541.10	-79 3.20	2047.85	977.523068	0.254	L	13.911	632.639	-224.409	978.082515	87.103	-137.307
265	90 8 1	-541.05	-79 3.20	2056.76	977.520627	0.320	L	13.838	635.388	-225.365	978.082500	87.353	-138.012
266	90 8 1	-540.99	-79 3.22	2044.46	977.524580	0.227	L	12.774	631.593	-224.046	978.082482	86.465	-137.581
267	90 8 1	-540.92	-79 3.25	2043.98	977.524873	0.280	L	12.407	631.445	-223.994	978.082461	86.264	-137.730
268	90 8 1	-540.84	-79 3.52	1939.58	977.547846	0.374	L	9.637	599.237	-212.780	978.082379	74.342	-138.438
269	90 8 1	-540.56	-79 3.45	1908.70	977.554553	0.200	L	9.425	589.711	-209.458	978.082355	71.334	-138.124
270	90 8 1	-540.51	-79 3.34	1956.59	977.544219	0.320	L	10.476	604.485	-214.608	978.082340	76.839	-137.789
271	90 8 1	-540.49	-79 3.24	2022.89	977.530426	0.414	L	11.525	624.939	-221.731	978.082334	84.356	-137.375
272	90 8 1	-540.41	-79 3.16	2053.47	977.525524	0.040	L	10.815	634.373	-225.012	978.082311	88.402	-136.611
273	90 8 1	-540.29	-79 3.13	2070.92	977.522089	0.120	L	10.880	639.756	-226.884	978.082275	90.430	-136.454
274	90 8 1	-540.17	-79 3.13	2109.17	977.512425	0.374	L	11.604	651.556	-230.985	978.082240	93.346	-137.638
275	90 8 3	-540.75	-79 3.66	1932.56	977.549296	0.093	L	9.431	597.072	-212.025	978.082241	73.387	-138.638
276	90 8 3	-540.84	-79 3.65	1916.60	977.552934	0.013	L	9.864	592.148	-210.308	978.082438	72.508	-137.800
277	90 8 3	-540.84	-79 3.71	1953.77	977.543125	0.187	L	11.343	603.615	-214.305	978.082438	75.645	-138.661
278	90 8 3	-540.81	-79 3.76	1941.31	977.546170	0.093	L	10.479	599.771	-212.966	978.082429	73.991	-138.974
279	90 8 3	-540.83	-79 3.80	1946.10	977.544169	0.013	L	11.508	601.249	-213.481	978.082435	74.491	-138.990
280	90 8 3	-540.75	-79 3.88	1930.83	977.548103	0.080	L	12.069	596.538	-211.839	978.082411	72.300	-139.539
281	90 8 3	-540.66	-79 3.93	1892.61	977.554693	0.280	L	10.392	564.747	-207.726	978.082384	67.448	-140.279
282	90 8 3	-540.52	-79 3.90	1808.79	977.574030	0.067	L	7.847	558.888	-198.696	978.082343	56.422	-140.273
283	90 8 3	-540.45	-79 3.85	1790.52	977.578167	0.013	L	7.322	553.252	-196.725	978.082322	56.418	-140.307
284	90 8 3	-540.40	-79 3.76	1803.46	977.575016	0.280	L	7.632	557.244	-198.121	978.082308	57.584	-140.537
285	90 8 3	-540.40	-79 3.65	1837.97	977.568590	0.0	L	7.752	567.890	-201.841	978.082308	61.925	-139.916
286	90 8 3	-540.42	-79 3.55	1876.30	977.561332	0.040	L	8.206	579.715	-205.970	978.082313	66.939	-139.032
287	90 8 3	-540.32	-79 3.88	1791.48	977.571222	0.067	L	8.056	553.548	-196.829	978.082284	56.442	-140.387
288	90 8 3	-540.22	-79 3.89	1777.81	977.579721	0.067	L	8.001	549.331	-193.354	978.082254	54.799	-140.536
289	90 8 3	-540.12	-79 3.93	1740.21	977.587061	0.053	L	8.403	537.731	-191.296	978.082225	50.970	-140.335
290	90 8 3	-540.07	-79 4.03	1694.56	977.595954	0.147	L	9.374	523.648	-186.364	978.082210	46.765	-139.539
291	90 8 3	-540.10	-79 4.13	1654.25	977.603667	0.067	L	9.392	511.212	-182.005	978.082219	42.051	-139.954
292	90 8 3	-540.14	-79 4.25	1664.45	977.601247	0.174	L	9.712	514.359	-183.109	978.082231	45.086	-140.022
293	90 8 3	-540.24	-79 4.31	1641.43	977.603349	0.027	L	9.553	507.257	-180.618	978.082260	40.698	-139.920
294	90 8 3	-540.33	-79 4.41	1636.56	977.609506	0.067	L	10.543	505.754	-180.091	978.082287	39.917	-140.174
295	90 8 3	-540.48	-79 4.38	1635.29	977.605991	0.200	L	10.072	505.363	-179.954	978.082331	40.094	-139.800
296	90 8 3	-540.60	-79 4.44	1606.84	977.612595	0.080	L	10.661	496.586	-176.874	978.082367	37.476	-139.399
297	90 8 3	-540.68	-79 4.54	1561.47	977.621267	0.013	L	10.838	482.589	-171.959	978.082390	32.304	-139.656
298	90 8 3	-540.60	-79 4.53	1517.23	977.629683	0.200	L	12.036	468.941	-167.162	978.082426	28.233	-138.929
299	90 8 3	-540.85	-79 4.44	1483.95	977.637127	0.107	L	12.032	458.674	-163.551	978.082441	25.392	-138.159
300	90 8 3	-540.90	-79 4.52	1455.09	977.642139	0.147	L	11.802	449.770	-160.417	978.082455	21.256	-139.161

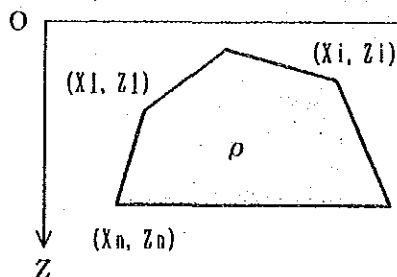
DENSITY = 2.67 (G/CM**3)

***** THE LIST OF GRAVITY SURVEY (PERU90) *****

ST.NO	OBS.DAY	LAT.	LONG.	LEVEL	ABS.G	C.20M	ETC	* LG *	TERR.C	F.E.C	B.G.C	NORM.G	ANOM.F	ANOM.B
301	90 718	-542.37	-79 4.73	1337.70	977.658242	0.227	L	LG *	17.046	413.555	-147.651	978.082891	5.952	-141.699
302	90 718	-542.22	-79 4.65	1297.68	977.666747	0.187	L	LG *	17.276	401.209	-143.292	978.082847	2.385	-140.907
303	90 718	-543.31	-79 3.24	1264.67	977.678049	0.013	L	LG *	13.868	391.025	-139.693	978.083171	-0.229	-139.922
304	90 718	-543.42	-79 3.43	1285.06	977.672693	0.027	L	LG *	15.778	397.316	-141.916	978.083204	2.582	-139.333
305	90 718	-543.57	-79 3.52	1309.75	977.667435	0.027	L	LG *	14.375	404.932	-144.607	978.083249	3.494	-141.113

with the measured gravity. The geometry of the disturbing body was then automatically adjusted from the starting model by using optimization techniques.

The gravitational attraction was calculated by Talwani's method, where the vertical component of the gravity, G_v , at an arbitrary point O on ground due to a polygon with a volume density ρ is given by following expression:



$$g_v = 2 \rho G \sum_{i=1}^n \int_{z_i}^{z_{i+1}} \int_{-\infty}^x \frac{Z}{X^2 + Z^2} dX \cdot dZ$$

where, ρ : density
 G : gravitational constant.

In the final analysis a multi-layered model based upon known geological structure was used. The results are shown in Fig.II-10(1), (2), (3), and (4).

1-1-6 Results of gravity data analysis

The analytical results obtained from this survey are presented in the following illustrations.

Fig. II-7 Bouguer Anomaly Map (2.67g/cm³).

Fig. II-8 First-order Residual Gravity Map.

Fig. II-9(1) Long-wave Gravity Map.

Fig. II-9(2) Short-wave Gravity Map.

Fig. II-10(1) Cross Section of A-A'.

Fig. II-10(2) Cross Section of B-B'.

Fig. II-10(3) Cross Section of C-C'.

Fig. II-10(4) Cross Section of D-D'.

Fig. II-11 Geophysical Interpretation Map.

1) Fig.II-7 Bouguer Anomaly Map (density=2.67g/cm³).

The Bouguer gravity in the survey area (Fig. II-1) is seen to vary from a low of -141 milligals (mgal) to a high of -136 mgal with a range of only 5 mgal. The maximum gravity gradient is 3 mgal/Km near Vista Alegre.

Major gravity highs are found in the central and north-eastern survey area with minor highs trending from Vista Alegre in the north to Tabacal in the south-east through the center of the area. The Bouguer gravity is found to be anomalously low along the south-eastern, southern, and south-western edges of the area. There are minor local lows in the interior of the area on the flanks of the major central high.

Most of the Bouguer highs occur on or near ridge lines with lows found in the valleys. An exception to this is seen near Los Laureles where a minor local high is located in a valley between two ridges and a minor low is located on a ridge. The Bouguer gravity contours conform roughly to topographic contours in the majority of the survey area, but there is only limited correlation between the two in the north-central quadrant of the area.

The Bouguer gravity values generally increase from the south-west to the north-east boundary of the survey area. This one-dimensional regional gravity trend is probably due to the influence of a broad geological structure at depth.

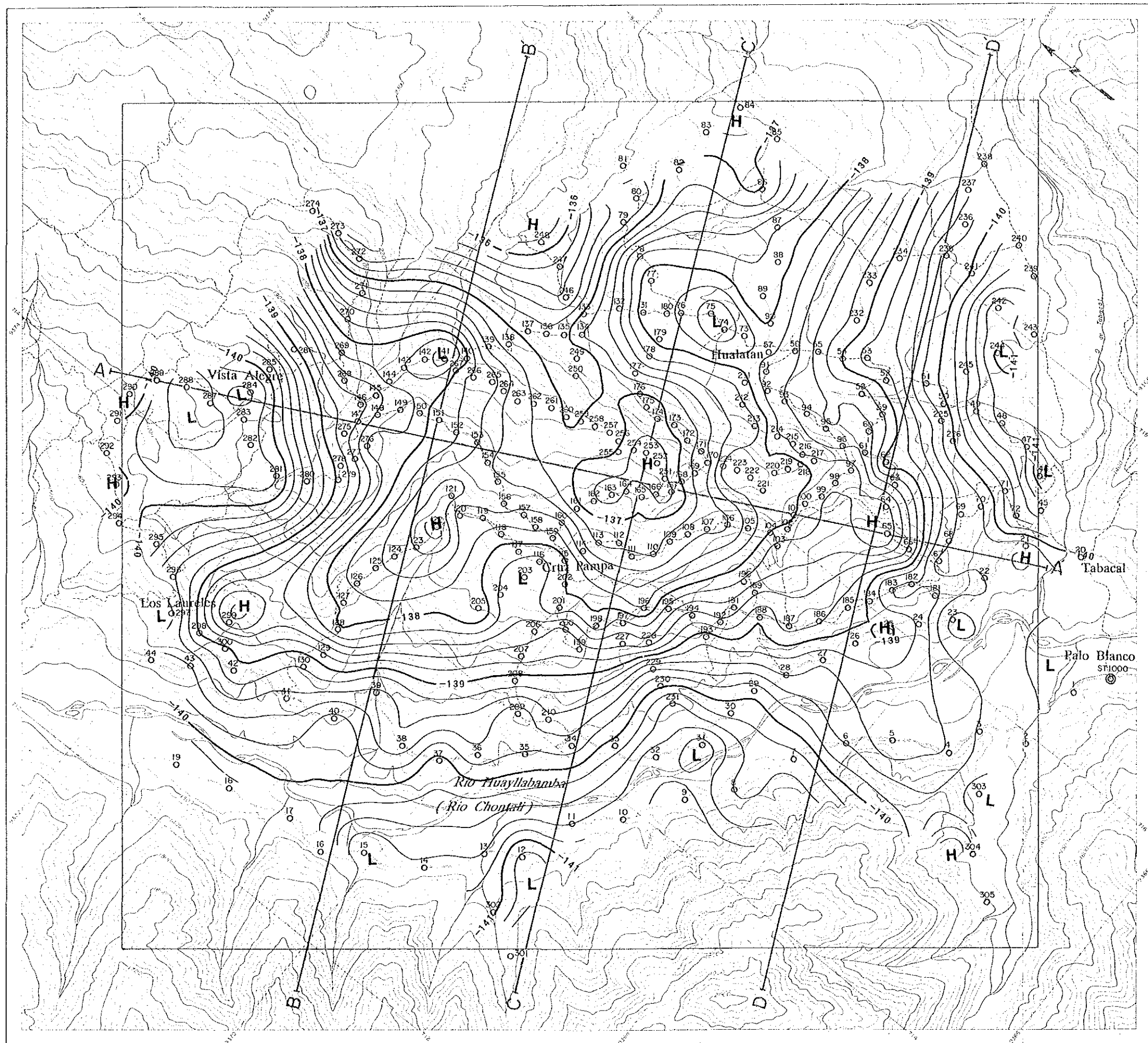
2) Fig.II-8 First-order Residual Gravity Map.

The first-order residual gravity map (Fig. II-8) is a representation of the residual gravity after removal of the one-dimensional regional gravity trend mentioned above. This data set represents the effect of shallow local features and ignores the effect of deep regional geological structures. There are only minor variations in the Bouguer Anomaly Map and the First-Order Residual Gravity Map. Residual gravity values range from a high of about 2.0 mgal to a low of -2.4 mgal. High residual gravity anomalies are observed in the middle of survey area, surrounded by low residual gravity zones. The gravity highs trend NNE-SSW and NW-SE through the center of the survey area.

The distribution of high and low residual anomalies may be summarized as follows:

i) A broad high residual anomaly is found in the middle of the survey area between Hualatan and Cruz Pampa with a maximum amplitude of about 2.0 mgal. Minor highs are distributed about the central high along conjugate axes running from NNE to SSW and from WNW to ESE through the center of the area. This distribution of highs may be the result of deformation and uplift of the basement rocks by regional conjugate stresses.

ii) There are low residual anomalies near Vista Alegre, north-east of Tabacal and along Rio Huallabanba. There is a granitic zone on the west side of Rio Huallabanba and, while granitic zones normally produce high gravity anomalies due to the relatively high density of granite, anomalously low values are



LEGEND

- O Gravity station
- A-A' Cross section
- 1.0 mgal interval
- 0.2 mgal interval
- H High gravity zone
- L Low gravity zone

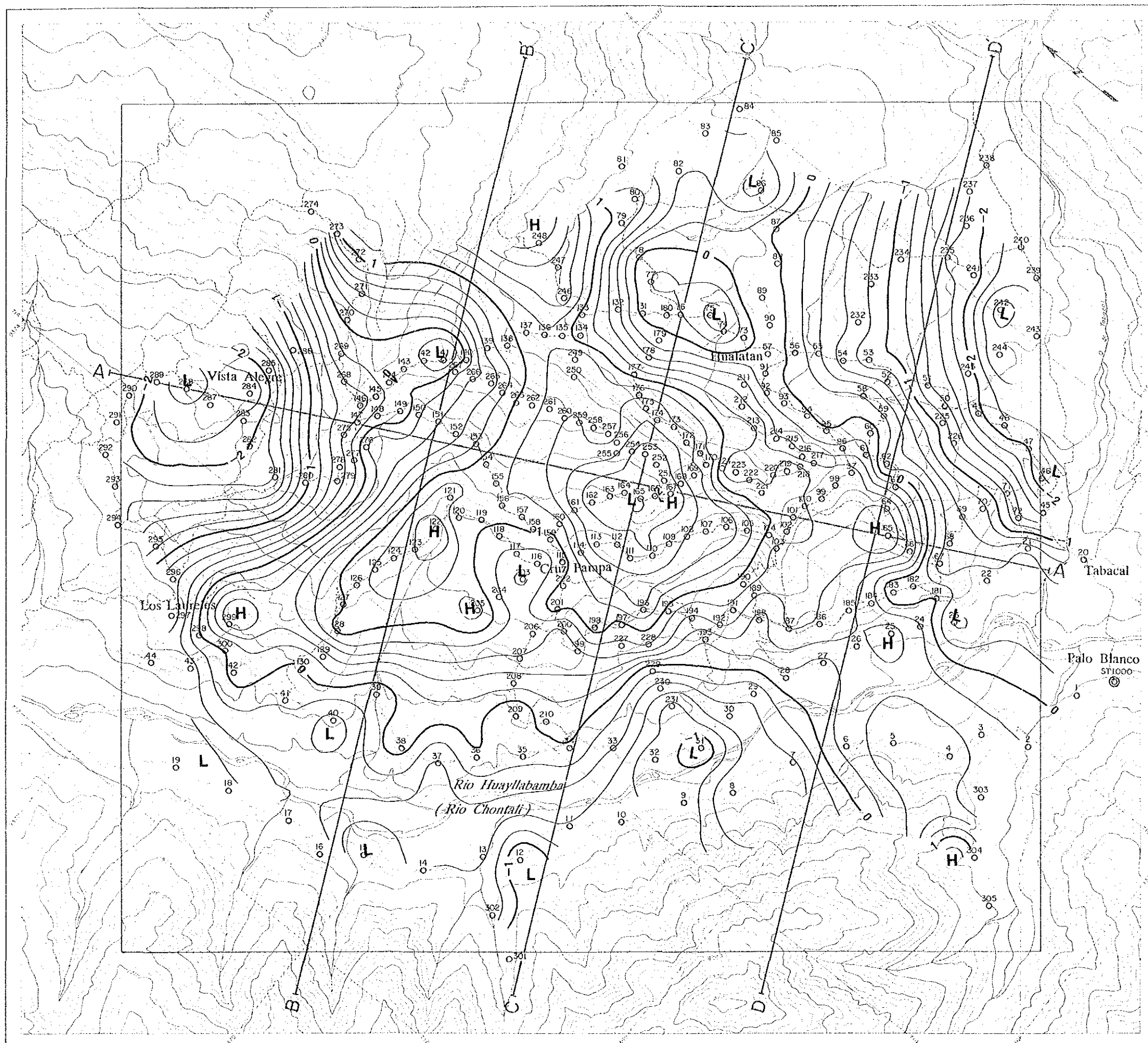
THE MINERAL EXPLORATION
 IN
 THE PACHAPIRIANA AREA
 REPUBLIC OF PERU
 (PHASE III)

GRAVITY SURVEY

Fig. II-7
 Bouguer Anomaly Map
 ($\rho = 2.67 \text{ g/cm}^3$)

FEBRUARY 1991





LEGEND

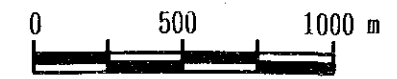
- Gravity station
- A-A' Cross section
- 1.0 mgal interval
- 0.2 mgal interval
- H High gravity zone
- L Low gravity zone

THE MINERAL EXPLORATION
 IN
 THE PACHAPIRIANA AREA
 REPUBLIC OF PERU
 (PHASE III)

GRAVITY SURVEY

Fig. II-8
 First-order
 Residual Gravity
 Map

FEBRUARY 1991



observed in this area.

3) Spectral analysis

The spectral behavior of the Bouguer gravity observed in the survey area will be analyzed in this section. The long-wave or low frequency variations in the gravitational field will be addressed first, then the short-wave or high frequency behavior of the field will be discussed.

(1) Fig.II-9(1) Long-wave Gravity Map.

The long-wave gravity map, Fig. II-9(1), generally shows variations in the gravity basement over the survey area. Values of long-wave gravity range from a low of minus 141.6 mgal in the south-west to a high of -136.8 mgal in the north-east. The high anomaly found at the north-eastern boundary of the survey area spreads to the south-west toward the middle of the area. The Bouguer gravity decreases from the center of the area to the south-east, south-west and north-west with a near constant gradient. Bouguer gravity values of less than -140 mgal occur on the west side of Rio Huallabanba, north-east of Tabacal, and north-west of Vista Alegre.

This implies that the gravity basement is shallow from the north-eastern quadrant to the center of the survey area and grows monotonically deeper to the south-east, south-west and north-west.

(2) Fig.II-9(2) Short-wave Gravity Map.

Local high and low short-wave gravity anomalies are distributed about the entire survey area, Fig. II-9(2). These anomalies reflect high and low density zones at a depth of about 170 meter below surface. The high short-wave gravity anomalies between Tabacal and Los Laureles are located on zones of anomalously high residual gravity, Fig. II-8. Remarkably high anomalies occur between Hualatan and Cruz Pampa, north-west of Tabacal and near Los Laureles. There is a high occurrence of quartz veins in the Hualatan and Cruz Pampa areas and this implies that high short-wave gravity anomalies may be correlated with mineralization.

There are numerous zones of anomalously low short-wave gravity in the Hualatan, Vista Alegre and Cruz Pampa areas which imply the probable presence of low density material at the surface.

4) 2 Dimensional simulation

In this section two-dimensional simulations derived from the processed gravity data will be addressed. The results of the simulations are presented in four illustrations, Fig.II-10(1-4). These illustrations include cross sections of the observed and calculated Bouguer gravity, Fig. II-10(1a), from which a one dimensional regional gravity trend has been removed by trial and error, long and short-wave gravity, Fig.II-10(1b), a density pseudosection, Fig. II-10(1c) and an assumed geological cross

section, Fig. II-10(1d). There are no control points to regulate the relative depth of gravity basement, such as deeply boring data. Therefore, the simulation was repeated until profile depths matched at points where sections lines crossed.

All sections were analyzed assuming a low density layer (2.67g/cm³) to overly a dense gravity basement (2.80g/cm³). From the data inversions, surface layers of anomalously low density (2.53-2.57g/cm³) and high density zones (2.80g/cm³) in the sub-surface were found to exist. While low density units are present at the surface, geological investigations show the presence of no high density host rocks or zones of locally high density at the surface. This implies that there are zones of anomalously high density in the sub-surface rocks.

The analyzed gravity basement or high density zones are denser than rock samples on Table II-2. This implies that base rock or sub-surface rock are mineralized such as highly carbonatized.

(1) Fig.II-10(1) Cross Section of A-A'

Cross section A-A' runs from north-west of Vista Alegre south-south-east to Tabacal, Fig.II-7.

The gravity basement (2.80g/cm³) lies at an elevation of about 1000 meters at the northern end of A-A' and rises at about 45x to around 1400m south-east of Vista Alegre (Fig. II-10(1)). Here there is a break in slope and the basement rises more gradually (>30') to crest at an elevation of 1700m near the intersection of lines A and C. From the intersection of lines A and C, the basement dips monotonically to the south-east toward Tabacal at about 30'.

A layer of low density material (2.54g/cm³) overlies the upper layer (2.67g/cm³) at the north end of line A and is as thick as 450m in the depression near Vista Alegre. This layer quickly thins to a veneer south-east of Vista Alegre but persists to the intersection of lines A and B.

A high density zone (2.80g/cm³), which extends nearly to the surface, is implied in the upper layer from the crest of the basement to the south of line C and another occurs at the intersection of lines A and D.

These zones of anomalously high densities may be the result of alteration of the unit by intrusion with the possibility of mineralization. These anomalies will be discussed further in the analysis of lines B, C and D.

(2) Fig.II-10(2) Cross Section of B-B'

Cross section B-B' strikes WSW-ENE in the northern half of the survey area, Fig.II-7.

The basement rocks lie at an elevation of 1100m along Rio Huayllabamba (Rio Chontali) at the west end of line B, Fig. II-10(2). They rise to the east to an elevation of 1550m, following topography to the midpoint of the line. The basement then dips to an elevation of 1400m east of the intersection of lines B and A, then rises at about 40' to an elevation of nearly 2Km near the

east end of the line.

A thin (<100m) low density (2.56g/cm³) surface layer covers the denser upper section along Rio Huayllabamba. Another low density zone develops near the intersection of lines B and C which thickens to 300m in the eastern half of the line. This layer pinches out near the topographic high at the east end of line B.

No high density zone were found in the upper layer of this section.

(3) Fig.II-10(3) Cross Section of C-C'

Cross section C-C' is parallel to B-B' and passes between Cruz pampa and Hualatan through the center of the survey area, Fig.II-7.

The general behavior of the basement along line C-C' is similar to line B. There is a basement low west of Rio Huayllabamba and the basement dome peaks with topography near the intersection of lines C and A. The west slope of the central basement dome is about 30' from horizontal and there is a depression east of the peak. The basement elevation at the east end of the line is only 1500m versus 1900m on line B and the east end of line C is flatter than line B.

The upper layer of line C is somewhat thicker than along line B (100-250m versus 50-200m). It is seen to thin on the flanks of the dome and thicken in the Rio Huayllabamba valley and north-east of Hualatan.

The low density units encountered along line B (2.56 and 2.54g/cm³) are present in profile C-C' (2.53g/cm³ and 2.55g/cm³). They overlay the upper layer west of Rio Huayllabamba and north of Hualatan. Both of these units have a maximum thickness of about 200m. The western unit has migrated out of the river valley to the west of rio Huayllabamba and the east-central unit has thinned from line B and begun to pinch out.

There is a high density zone (2.80g/cm³) in the upper layer near the center of line C, just east of the peak of the basement dome and beneath the topographic high of the line. This zone is in an area of known quartz vein occurrence and from its topographic relief appears to be erosion resistant.

(4) Fig.II-10(4) Cross Section of D-D'

Cross section D-D' parallels B-B' and C-C' near the southern boundary of the survey area, south of Hualatan and north of Tabacal, Fig.II-7.

The gravity basement has far less relief in this section than in the preceding two east-west cross sections and shows far less topographic control than on lines B and C, Fig. II-10(4). The basement elevation at the west end of the line, west of Rio Huayllabamba, is about 950m, which is comparable to its elevation on line C. It rises at about 10' to a maximum elevation of only 1250m near the intersection of lines A and D at the middle of line D. There is a basement syncline centered in the eastern half of profile D-D' with a trough depth of 900m.

The upper unit has thinned in the western half of the profile to a thickness of only 50 to 100m. In the eastern half of the line, however, it is as thick as 650m. This is a thickness comparable to that found in the depression north-west of Vista Alegre.

The low density unit observed on the west slope of the Rio Huayllabamba valley in cross section C-C' persists in profile D-D'. It has become marginally less dense (2.53g/cm³) and lies confined to the flank of steep topographic features to the west. The low density unit found near Hualatan on line C is not present in cross section D-D'.

The high density zone in the upper unit of line C, at the crest of the basal anticline, is again encountered in cross section C-C' and it again occurs upon a basement high. A second zone of high density has developed as well. It lies to the east of the basement crest and both of these zones have densities of 2.80g/cc.

5) Fig. II-11 Geophysical Interpretation Map

In the interest of developing an integrated geophysical interpretation, a geophysical interpretation map was developed, Fig. II-11. This map incorporates the results of this gravity survey and those of the Controlled Source Audio Magnetotellurics (CSAMT) survey performed in this area in 1989.

The data sets presented in this illustration are:

a) A contour map of the elevation of the gravity basement relative to mean sea level.

b) (Assumed) Zones of anomalously high densities.

{ data sets a) and b) were derived from this set of gravity data by two dimensional simulation }

c) Areas determined to have resistivities higher than 1,000 ohm-m.

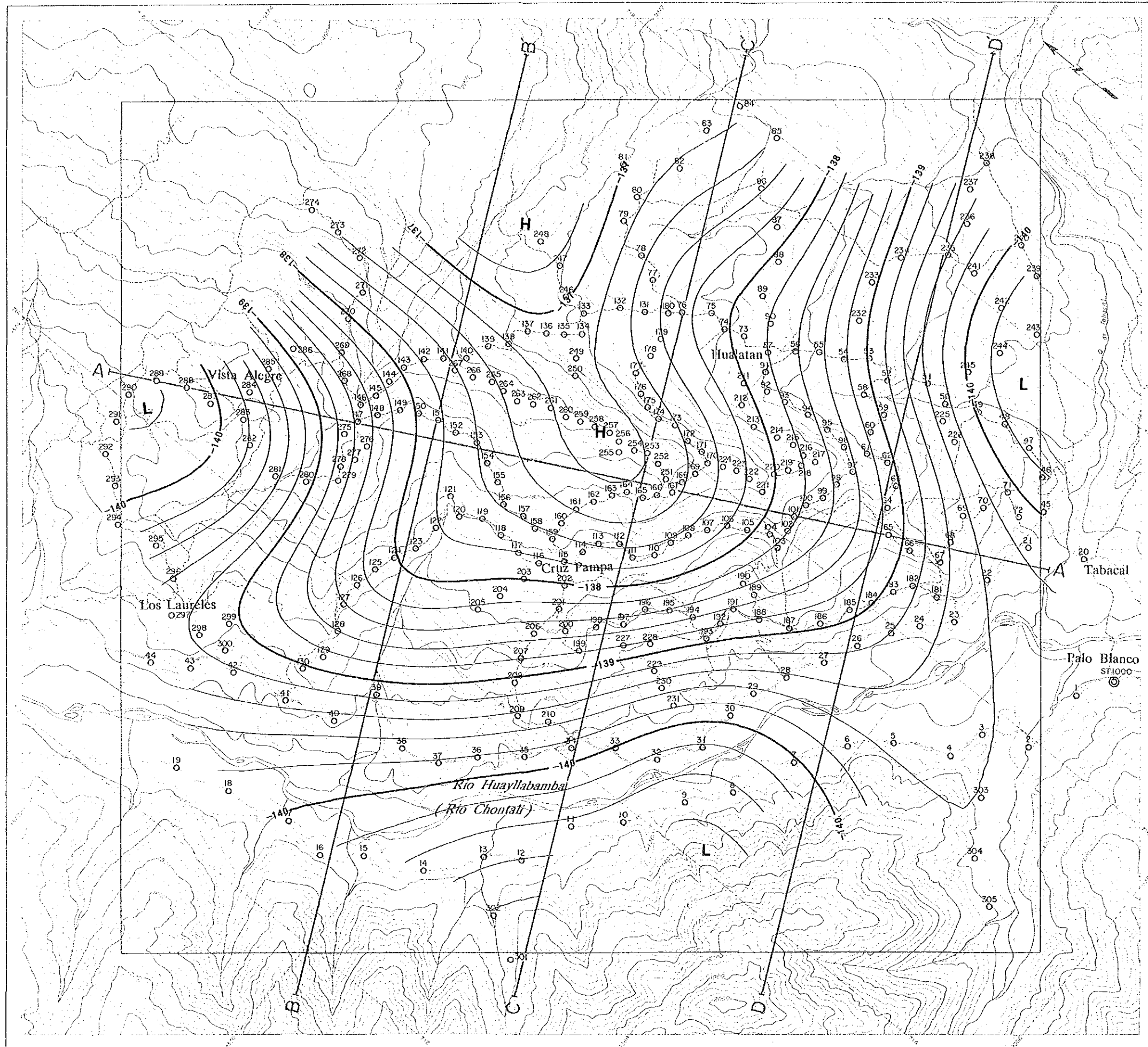
d) Zones with resistivities lower than 20 ohm-m.

{ data sets c) and d) were derived from the CSAMT data contoured at an elevation of 1600m above sea level. }

e) Quartz veins are indicated as solid black lenses.

The basement depth map presented in Fig. II-11 is quite similar in shape to the long-wave gravity map, Fig. II-9(1). The gravity basement forms a closed dome at the center of the survey area where it is about 100m beneath the surface at an elevation of 1700m. There is a minor syncline in the basement to the north-east of the dome which plunges to the south-east in the direction of Hualatan and to the north-west toward Vista Alegre. The basement rises beyond the syncline in the north-eastern quadrant of the survey area to its maximum elevation in excess of 1700m above sea level. The gravity basement reaches lows west of Vista Alegre and south-west of Rio Huayllabamba where it drops to less than 900m above sea level.

A shallow zone of high density was found in the upper layer slightly south-east of the peak of the basement dome. Two more high density anomalies occur on the south-eastern flank of the



LEGEND

- O Gravity station
- A-A' Cross section
- 1.0 mgal interval
- 0.2 mgal interval
- H High gravity zone
- L Low gravity zone

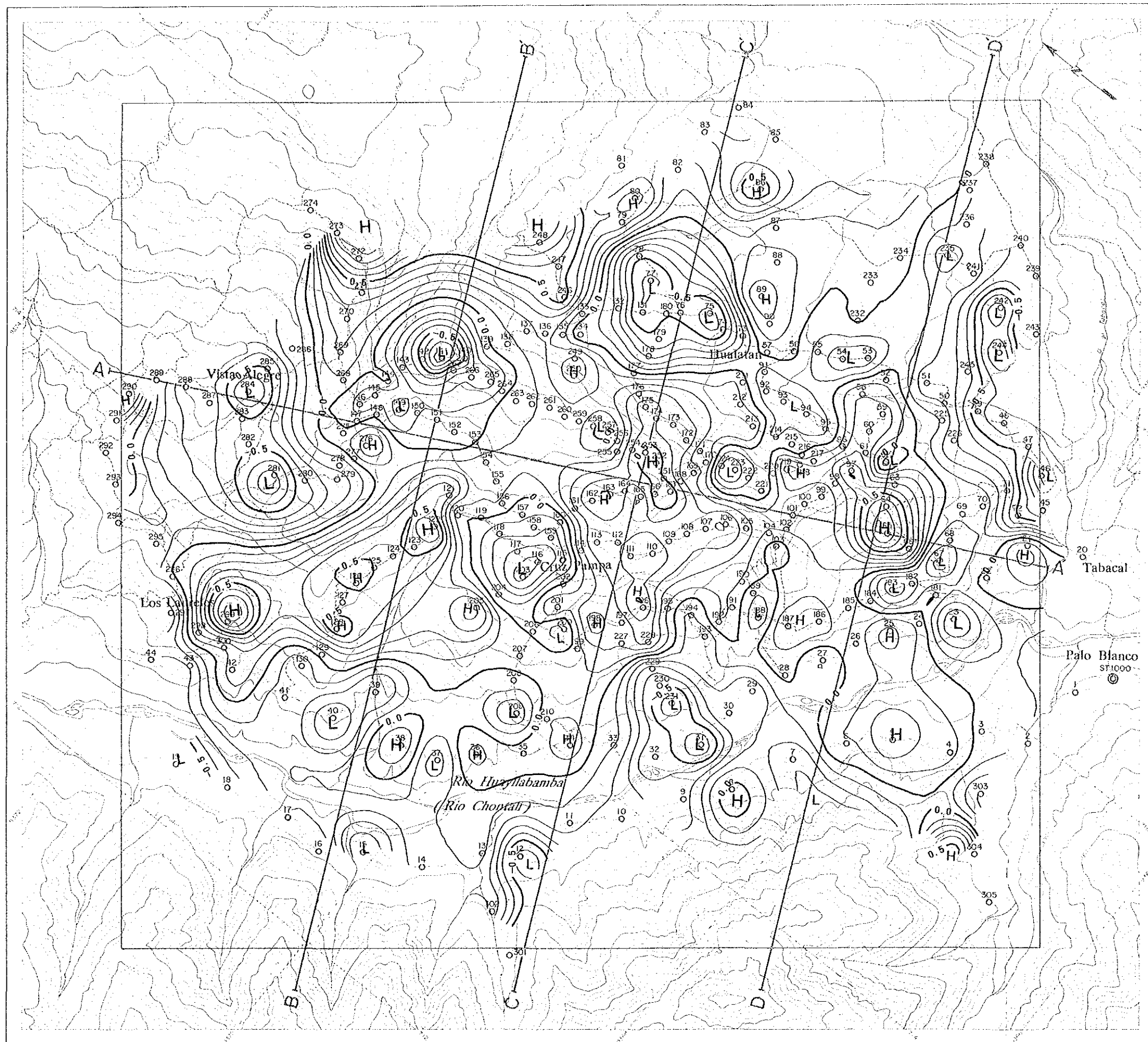
THE MINERAL EXPLORATION
IN
THE PACHAPIRIANA AREA
REPUBLIC OF PERU
(PHASE III)

GRAVITY SURVEY

Fig. II-9 (1)
Long-wave
Gravity Map

FEBRUARY 1991





LEGEND

- Gravity station
- A-A' Cross section
- 0.5 mgal interval
- - - 0.1 mgal interval
- H High gravity zone
- L Low gravity zone

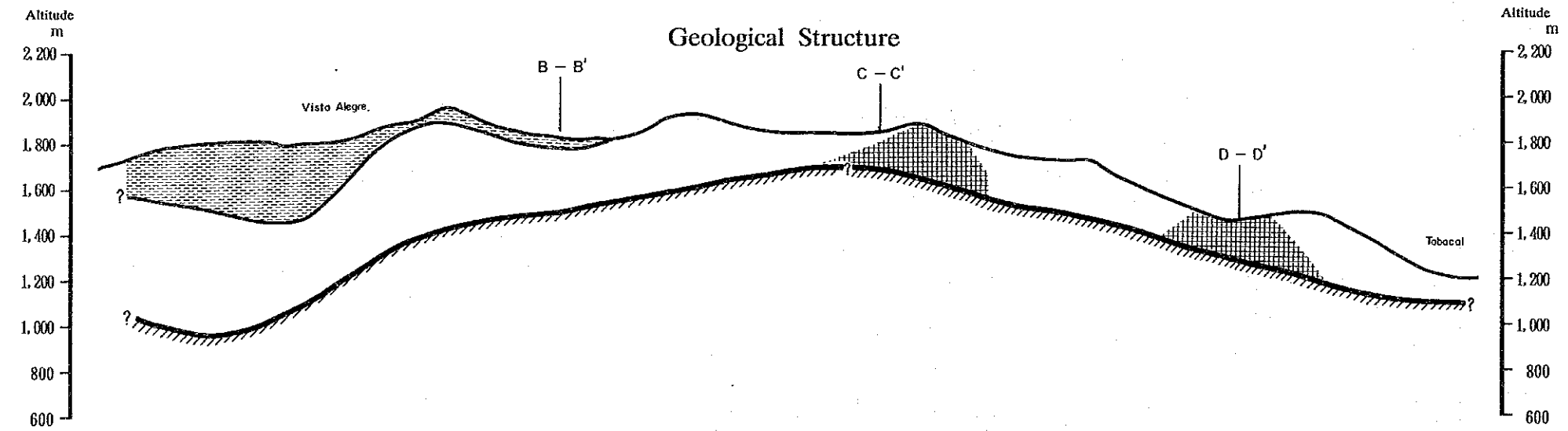
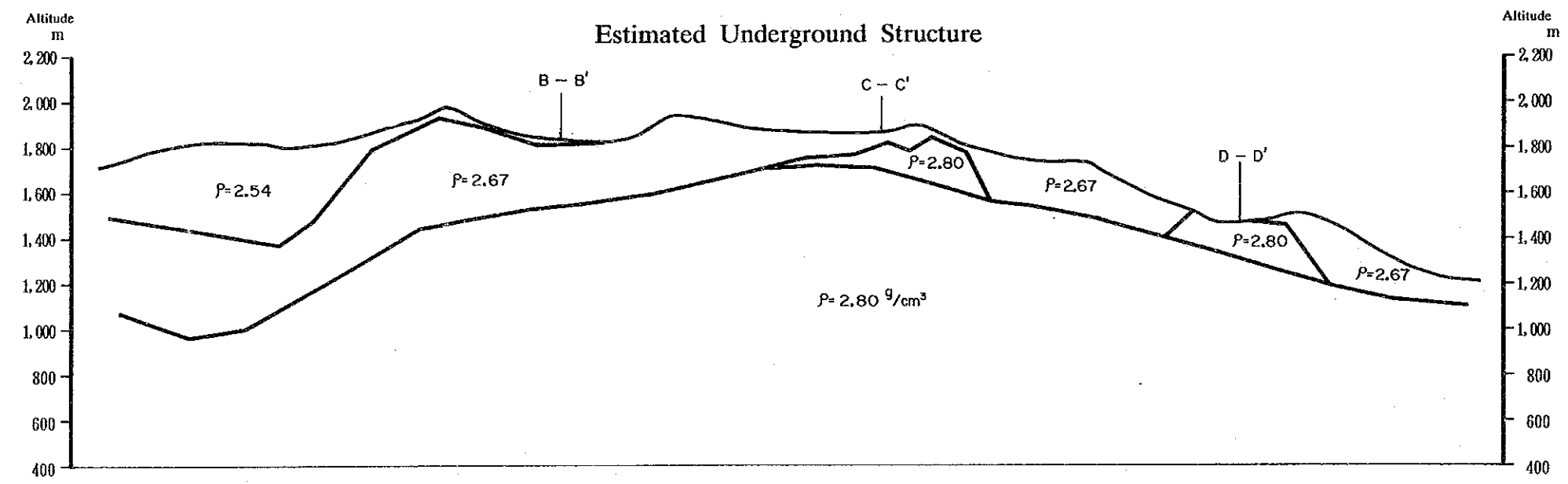
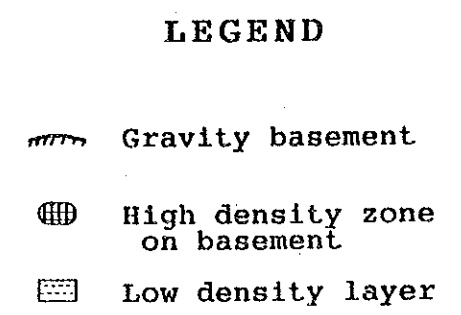
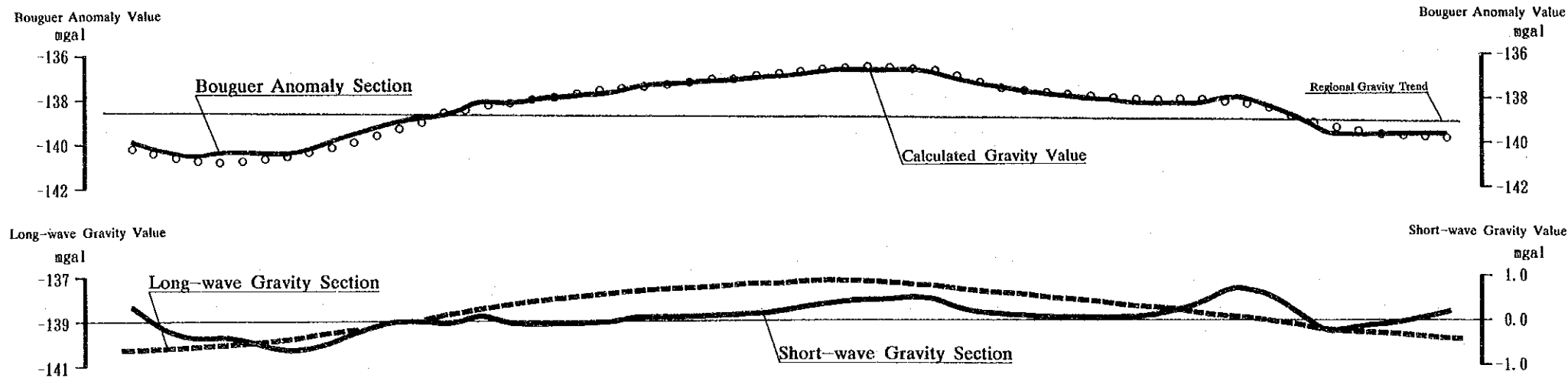
THE MINERAL EXPLORATION
 IN
 THE PACHAPIRIANA AREA
 REPUBLIC OF PERU
 (PHASE III)

GRAVITY SURVEY

Fig. II-9 (2)
 Short-wave
 Gravity Map

FEBRUARY 1991





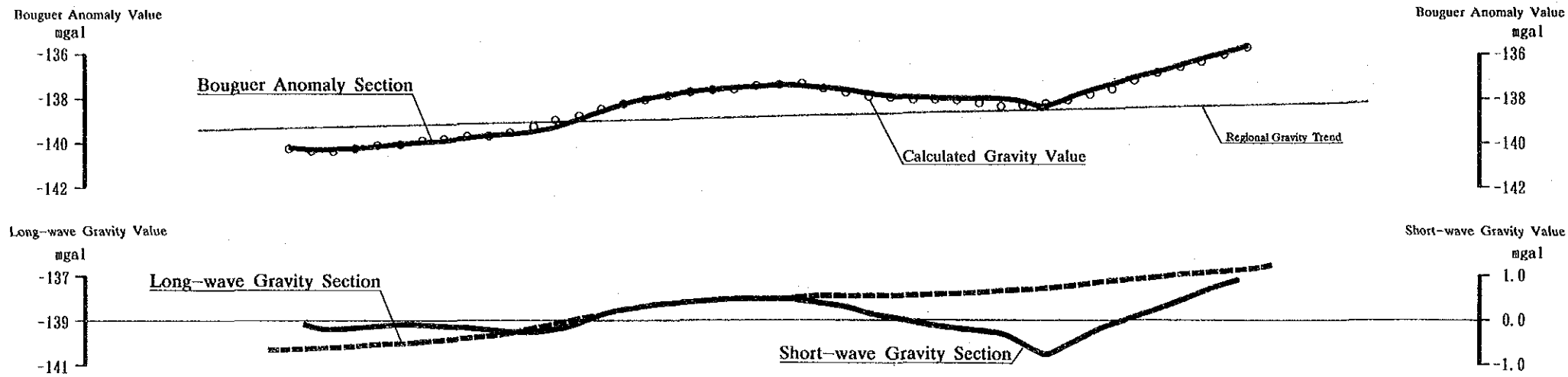
THE MINERAL EXPLORATION
IN
THE PACHAPIRIANA AREA
REPUBLIC OF PERU
(PHASE III)

GRAVITY SURVEY

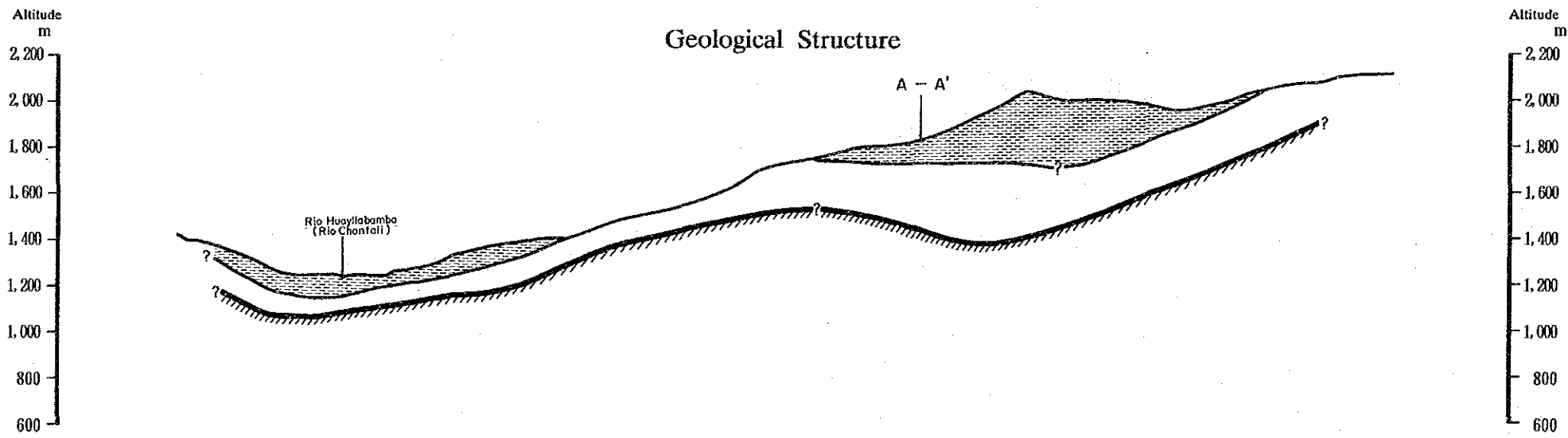
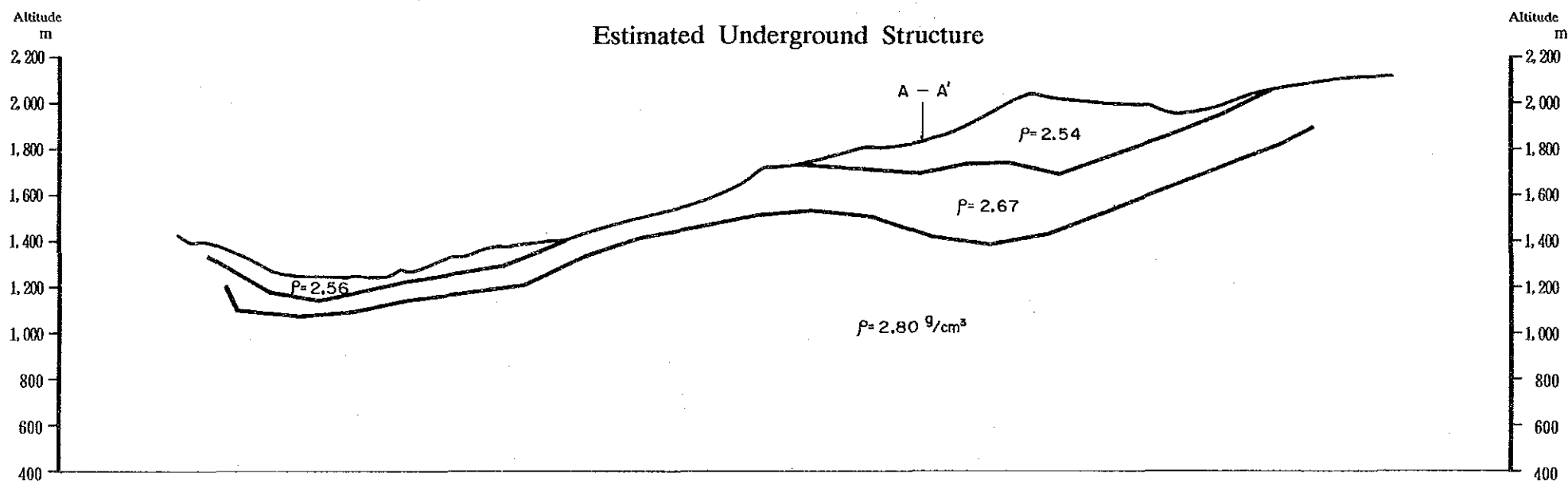
Fig. II-10 (1)
Cross Section
of A-A

FEBRUARY 1991

0 500 1000 m



- LEGEND**
- Gravity basement
 - High density zone on basement
 - Low density layer



THE MINERAL EXPLORATION
IN
THE PACHAPIRIANA AREA
REPUBLIC OF PERU
(PHASE III)

GRAVITY SURVEY

Fig. II-10 (2)
Cross Section
of B-B

FEBRUARY 1991

